SEDIMENTOLOGY AND STRATIGRAPHY OF THE MIOCENE-PLIOCENE

BOUSE FORMATION NEAR CIBOLA, ARIZONA AND MILPITAS WASH,

CALIFORNIA: IMPLICATIONS FOR THE EARLY EVOLUTION OF THE

COLORADO RIVER

by

MINDY BETH HOMAN

A THESIS

Presented to the Department of Geological Sciences
and the Graduate School of the University of Oregon
in partial fulfillment of the requirements
for the degree of
Master of Science

December 2014

THESIS APPROVAL PAGE

Student: Mindy Beth Homan

Title: Sedimentology and Stratigraphy of the Miocene-Pliocene Bouse Formation near Cibola, Arizona and Milpitas Wash, California: Implications for the Early Evolution of the Colorado River

This thesis has been accepted and approved in partial fulfillment of the requirements for the Master of Science degree in the Department of Geological Sciences by:

Dr. Rebecca J. Dorsey	Chairperson
Dr. Gregory J. Retallack	Member
Dr. Marli B. Miller	Member

and

J. Andrew Berglund	Dean of the Graduate School

Original approval signatures are on file with the University of Oregon Graduate School.

Degree awarded December 2014

THESIS ABSTRACT

Mindy Beth Homan

Master of Science

Department of Geological Sciences

December 2014

Title: Sedimentology and Stratigraphy of the Miocene-Pliocene Bouse Formation near
       Cibola, Arizona and Milpitas Wash, California: Implications for the Early
       Evolution of the Colorado River

The ~5.6-4.8 Ma Bouse Formation, exposed along the lower Colorado River,
contains a well exposed but debated record of river integration. Sedimentologic and
stratigraphic analysis aid interpretation of depositional processes, relative water depth,
depositional environments, stratal architecture, and basin-filling history. Data collected
include detailed measured sections, facies descriptions, and fault measurements. Seven
lithologically distinct units have been identified along with numerous marine sedimentary
structures and fossils. The Bouse Formation preserves a systematic sequence-
stratigraphic architecture that records two cycles of base level rise and fall. Lacustrine
versus estuarine interpretation remains elusive, though new isotope and
micropaleontology data suggest a shift from marine to lacustrine. Constructed
stratigraphic facies panels reveal a wedging geometry indicative of syn- to post-
depostional tilting, leading us to propose a "sag basin" model during deposition of the
Bouse. Finally, the newly described Bouse upper limestone unit resolves a long-standing
debate over the age of the first through-going river.

CURRICULUM VITAE

NAME OF AUTHOR: Mindy Beth Homan

GRADUATE AND UNDERGRADUATE SCHOOLS ATTENDED:

      University of Oregon, Eugene
      Miami University, Oxford, Ohio

DEGREES AWARDED:

      Master of Science, Sedimentology and Stratigraphy, 2014, University of Oregon
      Bachelor of Science, Geology, 2012, Miami University

AREAS OF SPECIAL INTEREST:

      Sedimentology
      Stratigraphy
      Basin Analysis
      Petroleum geology
      Structural geology
      Geologic mapping
      Paleontology

PROFESSIONAL EXPERIENCE:

      Paleontologist/IT Specialist Intern, Dinosaur National Monument, May-August
         2012

      Petroleum Geoscientist Intern, Devon Energy Corporation, June-Sept. 2014

      Graduate Teaching Fellow, University of Oregon, 2012 to present

GRANTS, AWARDS, AND HONORS:

      Graduate Student Research Grant, Geological Society of America, 2013

PUBLICATIONS:

Dorsey, R.J., Crossey, L.J., Cohen, A.S., Howard, K.A., Karlstrom, K.E., Bright, J., Homan, M., Mcdougall, K., and Retallack, G.J., 2013, Lake-estuary hypothesis for the Bouse Formation: New look at an old problem, GSA *Abstracts with Programs*. Vol. 45, No. 7, p. 253.

Homan, M.B. and Dorsey, R.J., 2013, Sedimentology and stratigraphy of the southern Miocene-Pliocene Bouse Formation, GSA *Abstracts with Programs*. Vol. 45, No. 7, p. 607.

Barrett, H.A., Homan, M.B., and Krekeler, M.P.S., 2012, Geologic education and assessment with a new rock and mineral specimen display, GSA *Abstracts with Programs*. Vol. 44, No. 7, p. 100.

Currie, B.S., McPherson, M.L., Hokanson, W., Pierson, J.S., Homan, M.B., Pyden, T., Schellenbach, W., Purcell, R., and Nicklaus, D.H., 2012, Reservoir characterization of the Cretaceous Cedar Mountain and Dakota Formations, northern Uinta Basin, Utah and Colorado. Utah Geological Survey Open-File Report 597, 81 p.

Currie, B.S., McPherson, M.L., Pierson, J.S., Dark, J.P., Hokanson, W.H., Homan, M.B., Purcell, R.M., Pyden, T.J., and Schellenbach, W.L., 2011, Sequence stratigraphy of the mid-Cretaceous Dakota Formation and Mowry Shale, Uinta Basin, Utah and Colorado, GSA *Abstracts with Programs*. Vol. 43, No. 5, p. 602.

ACKNOWLEDGMENTS

First of all, I wish to express sincere thanks and appreciation to Dr. Rebecca Dorsey, my rock and my guide on this journey. Dr. Dorsey not only assisted me through over two years of master's thesis work, but she also shared with me her spirit and enthusiasm for sedimentology/stratigraphy and the Bouse Formation, shaping me into the geologist I am today. It is with great joy that I present this masterpiece on the enigmatic Bouse Formation. In addition, I owe a special thanks to Dr. Marli Miller and Gregory Retallack for their guidance and support with the project. Lastly, I would like to thank my field assistants over the past two years, Chris Pope, Kevin McCarten, and Michael Thomas, who were with me every step of the way and have probably climbed on every outcrop of the Bouse Formation in existence.

My family has also been an important component in the completion of this thesis. It is with their continued love and support that I move on to the next chapter of my life and I am able to close this one, with them always cheering in the background. Michael Thomas, the love of my life, has stood by me every single step of the way through my M.S. thesis journey and a million more steps will we hopefully share together in the future. Thank you for always being there, through thick and thin; I realize dating a geology graduate who spends many months in the field each year has been quite the unique challenge.

Finally, this research was supported by the University of Oregon, Department of Geological Sciences and a Graduate Student Research Grant from the Geological Society of America.

TABLE OF CONTENTS

Chapter	Page

LIST OF FIGURES

LIST OF TABLES

CHAPTER I

INTRODUCTION

The Miocene-Pliocene Bouse Formation, exposed discontinuously along the lower Colorado River in California and Arizona, records integration of the early Colorado River and its initial connection to the Gulf of California (Fig 1). Exposures of the Bouse Formation occupy the southernmost "paleolake Blythe" (Spencer et al., 2008), and provide insights into the conditions and processes that culminated in integration of this large river system. The record of initiation and integration of the Colorado River is widely debated due to conflicting data and incompatible models for the Bouse Formation. Our understanding of how and when the Colorado River became linked to the Gulf of California depends on interpretation of the Bouse Formation, where debate is focused on whether the southern Bouse accumulated in a marginal-marine estuary or a series of large, inland lakes isolated from the ocean. Marine fossils and lithofacies provide evidence for deposition in a restricted marine-estuary environment (e.g. Metzger, 1968; Smith, 1970; Buising, 1990; McDougall, 2008), but Sr-isotope studies support a lacustrine origin for Bouse carbonate and conclude that marine fossils were introduced by avian transport (birds) (Spencer and Patchett, 1997; Spencer et al., 2008; Roskowski et al., 2010).

Understanding of Bouse deposition is also important for constraining the timing and amount of uplift of the western Colorado Plateau region. If the Bouse accumulated in a marine estuary, it would require uplift of ~300-500 m since 5 Ma. If it was deposited in a chain of lakes, no late Cenozoic uplift is required, and the modern regional topography would date to Pliocene-Quaternary time (Spencer and Patchett, 1997).

1
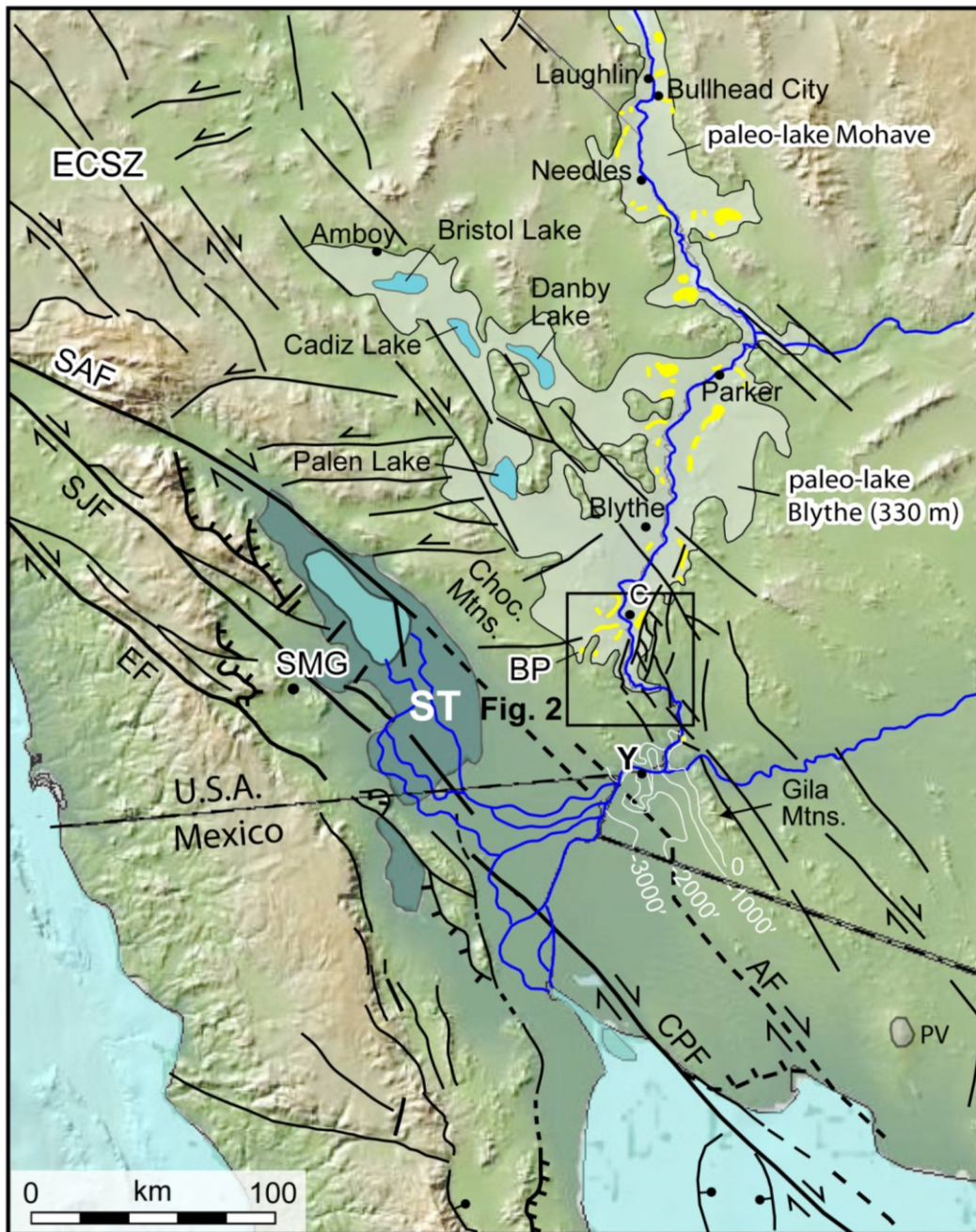
Figure 1. Map of the lower Colorado River region and surrounding areas. Surface exposures of the Bouse Formation are indicated in yellow. Paleo-lake maximum elevations modified from Spencer et al. (2008). White lines south of Yuma are subsurface structure contours showing elevation (in feet) of the top of the Bouse Formation (Olmsted et al., 1973). Locations: BP, Buzzards Peak; C, Cibola; P, Parker; PV Pinacate volcano; SMG, Split Mountain Gorge; ST, Salton Trough; Y, Yuma. Faults: CPF, Cerro Prieto fault; ECSZ, eastern California shear zone; EF, Elsinore fault; SAF, San Andreas fault; SJF, San Jacinto fault.

2

Early studies proposed that the Bouse Formation was deposited in a marine estuary at the north end of the Gulf of California rift, followed by first arrival of the through-going Colorado River and progradation of the earliest river-delta sediments into the marine embayment (Metzger, 1968; Smith, 1970; Winterer, 1975; Buising, 1988, 1990). An alternative hypothesis proposes that the Bouse was deposited in a series of linked inland lakes filled by the Colorado River and isolated from the ocean, as indicated by Sr, C, and O isotope data (Spencer and Patchett, 1997; Poulson and John, 2003; Roskowski et al., 2010; Spencer et al., 2011). A third, hybrid lake-estuary hypothesis, postulates that nonmarine lakes in the north were linked to a large marine estuary in the south with intermittent connections to the ocean and that complex mixing in the southern paleo-lake Blythe produced large fluctuations in water chemistry, salinity, depositional processes, environments, and faunas (Dorsey et al., 2013; Crossey et al., 2011, 2013).

This study investigates the detailed stratigraphy and sedimentology of the Bouse Formation in southern paleo-lake Blythe (Fig. 2), to reconstruct changes in depositional processes and environments through time and better understand the tectonic and climatic controls on basin evolution. We combine measured sections, detailed sedimentary lithofacies descriptions, subsurface data, fault measurements, and stratigraphic panels to reconstruct the evolution and deposition of the Bouse Formation during initiation and integration of the Colorado River. This analysis allows us to test hypotheses for Bouse depositional environments and stratigraphic architecture, and better understand the latest Miocene to early Pliocene evolution of the southernmost Colorado River corridor.

3

Figure 2. Geologic map of the lower Colorado River region from the Palo Verde Mts to the eastern Chocolate Mountains (compiled from Sherrod and Tosdal, 1991; Richard, 1993, Ricketts et al., 2011). Most faults have been relatively inactive since ~6 Ma, but some cut the Bouse Formation south and SE of Cibola. Dashed wide white line is the inferred paleodam of Spencer et al. (2008).

4

CHAPTER II

GEOLOGIC SETTING AND REGIONAL STRATIGRAPHY

The lower Colorado River Valley extends from the mouth of the Grand Canyon, along the border between southern California and Arizona, to Yuma where the river enters the Salton Trough basin (Fig. 1). The lower Colorado River Valley contains a complex geologic record of Miocene to Quaternary extension accompanied by wrench tectonics and strike-slip faulting in the nearby Eastern California Shear Zone (ECSZ), a dextral shear zone located east of the San Andreas Fault System (Fig. 1).

Lower Colorado River Valley

Deposits older than ~6.0 Ma around and south of Lake Mead pre-date arrival of the Colorado River in the lower Colorado River corridor (Lucchitta, 1972, 1979; Spencer et al., 2001; Pederson, 2008; House et al., 2008). During early Tertiary to early Miocene time, regional rivers flowed north and northeast away from previously uplifted Laramide deposits in the present-day Basin-and-Range province across the Colorado Plateau (Lucchitta, 1972, 1979; Young, 1979; Potochnik, 2001). Basin-and-range extension starting at ~18 Ma caused tectonic lowering of topography and reversal of the regional drainages. Sedimentary deposits in the Lake Mead area record a pronounced switch from low-energy deposition in middle to late Miocene internally drained basins to arrival of the through-going Colorado River soon after deposition of the Late Miocene (12–6 Ma) Hualapai Limestone (Spencer et al., 2001; Pederson, 2008).

The age of the Bouse Formation is bracketed between ~ 5.6 and 4.8 Ma, and thus spans the age of initiation of the Colorado River. Near Bullhead City (Fig. 1), basal Bouse limestone overlies and slightly post-dates the 5.6-Ma tuff of Wolverine Creek

(House et al., 2008). Near Buzzards Peak in the south, Bouse carbonate is interbedded with the 4.8 Ma Lawlor tuff (Sarna-Wojcicki et al., 2011; Harvey 2014). It is widely recognized that the through-going Colorado River was well established after deposition of the Bouse Formation (e.g. House et al., 2008). In addition, stratigraphic evidence suggests that river sediment prograded down the lower Colorado River valley to the Salton Trough *during* deposition of the Bouse (e.g., Buising, 1988, 1990), first arriving in the Salton Trough at 5.3 Ma (Dorsey et al., 2007, 2011). Alternatively, some models propose that the through-going river system was not established until after deposition of the youngest Bouse in the south, and thus should be younger than 4.8 Ma (e.g., Spencer et al., 2013). The modern Colorado River is inset into the Bouse Formation and other basin-fill deposits of the lower Colorado River valley (Figs. 1, 2).

Regional Structure and Deformation History

The Eastern California Shear Zone (ECSZ) is a broad zone of dextral faults and block rotations located east of the San Andreas Fault system that cuts across the lower Colorado River valley (Fig. 1) and continues north into Nevada (Glazner et al., 2002; Shelef and Oskin, 2010). The ECSZ underwent regional extension in early Miocene time, 24-23 Ma to 18.5 Ma (Howard and Miller, 1992; Jachens and Howard, 1992; Glazner et al., 2002). Younger strike-slip faulting and transpression of the ECSZ is related to the evolution of the San Andreas Fault system during reorganization of the transform plate boundary (Bartley and Glazner, 1991). When extension of the ECSZ ended ca. 18.5 Ma, deformation in the Mojave Desert continued as strike-slip faulting and transpression (Glazner et al., 2002; Shelef and Oskin, 2010). Dextral faulting persisted until Pleistocene and Holocene time, and the Mojave block has continued to

accommodate deformation through strike-slip faulting to the present day (Howard and Miller, 1992; Jachens and Howard, 1992; Glazner et al., 2002; Shelef and Oskin, 2010).

Early to middle Miocene extension along the lower Colorado River Valley created regional low-angle detachment faults and related core complexes and extensional basins that became inactive around 12-14 Ma (Davis and Lister, 1988; Spencer and Reynolds, 1989; Nielson and Beratan, 1990; Dorsey and Becker, 1995). Orocopia Schist is present in the footwalls of several middle Tertiary extensional detachment faults that cut strongly tilted upper-plate Miocene volcanic rocks in the Chocolate Mountains (Fig. 2). The low-angle detachment faults are cut and offset by younger high-angle normal faults of the Laguna Fault System, which were active during late Miocene (ca. 12-6 Ma) strike-slip faulting in the ECSZ and related folding in the Chocolate Mountains (Sherrod and Tosdal, 1991; Richard, 1993; Ricketts et al., 2011). Normal faults and strike-slip faults in the Trigo Mountains (Fig. 2) bound a series of small basins and flanking uplifts that make up the en-echelon transtensional Laguna Fault System of Richard (1993), which connects southeastward to dextral strike-slip faults in Mexico (Fig. 1). Fault truncation of the Bouse Formation south of Cibola shows that some of these faults clearly have an additional history of younger offset (Sherrod and Tosdal, 1991). Post-Miocene strain on these faults is minor compared to older Miocene extensional and wrench deformation, but the Pliocene-Pleistocene history of slip on these faults is little studied and poorly understood.

Regional Stratigraphy

The Bouse Formation varies considerably from north to south along the lower Colorado River valley. North of paleolake Blythe, the Bouse Formation consists of a thin

basal limestone with very rare to no fossils, overlain by interbedded lacustrine to deltaic mudstone, siltstone, and sandstone (Metzger, 1968; Buising, 1990; House et al., 2008). Farther south in the Parker-Blythe-Cibola area (paleolake Blythe), outcrops totaling about ~70 m in thickness reveal a much thicker and lithologically diverse basal limestone unit that includes abundant marine fossils and high-energy bioclastic facies. Bioclastic facies and marine fossils are only found in the southern paleolake Blythe (Metzger, 1968; Buising, 1990; Spencer et al., 2013). In this southern area, the Bouse is considered to consist of three main facies (1) Thin fossiliferous basal limestone, which includes marl, fossil hash, and calcarenite; (2) Interbedded claystone, sandstone, and mudstone; and (3) basin margin facies of massive tufa and travertine encrusting onto bedrock (Buising, 1988, 1990). Surface outcrops of Bouse Formation disappear further south; however, Bouse measured in the subsurface ~1000 m below, near Yuma, AZ, reaches thicknesses of up to >660 m (Metzger, 1968; Spencer and Patchett, 1997; Lucchitta et al., 2001).

The Bouse Formation rests unconformably on either (1) Miocene alluvial fan sediments known as "fanglomerate" or (2) older Miocene volcanic rocks. The fanglomerate was deposited as a local basin fill during rifting that took place prior to Bouse deposition and arrival of the Colorado River (Lucchitta, 1972; House et al., 2008; Spencer et al., 2008, 2013). The fanglomerate consists primarily of poorly sorted sandy conglomerate and pebbly sandstone with clasts of volcanic and intrusive rocks, and exhibits weak, pervasive horizontal stratification. The early Miocene volcanics are generally pink, green, white, purple, or brown rhyolites, dacites and andesites.

Erosionally overlying and inset into the Bouse is the aggradational Bullhead Alluvium and younger units such as the Quaternary Terrace gravels. The Bullhead

Alluvium is erosionally inset into the Bouse about 200 meters and dates to ~4.5-3.5 Ma (House et al.,2008; Howard et al., 2008). The Bullhead Alluvium contains distinctive well rounded, pink Colorado River sand, well rounded quartzite and chert clasts, and occasional clasts of reworked Bouse carbonate. The Bullhead Alluvium is interpreted to represent the earliest deposits of the through-going Colorado River (House et al., 2008; Howard et al., 2008).

Figure 3 illustrates a simple nomenclature for the lithofacies and general stratigraphy of the Bouse Formation that builds on previous studies (Metzger, 1968; Buising 1990, 1993). We subdivide the Bouse into well-defined facies that permit systematic mapping and analysis of this formation (Fig. 3). Work done in previous studies defined three main facies for the Bouse Formation: basal carbonate, basin-margin carbonate, and interbedded unit. In this study, we recognize those basic subdivisions and
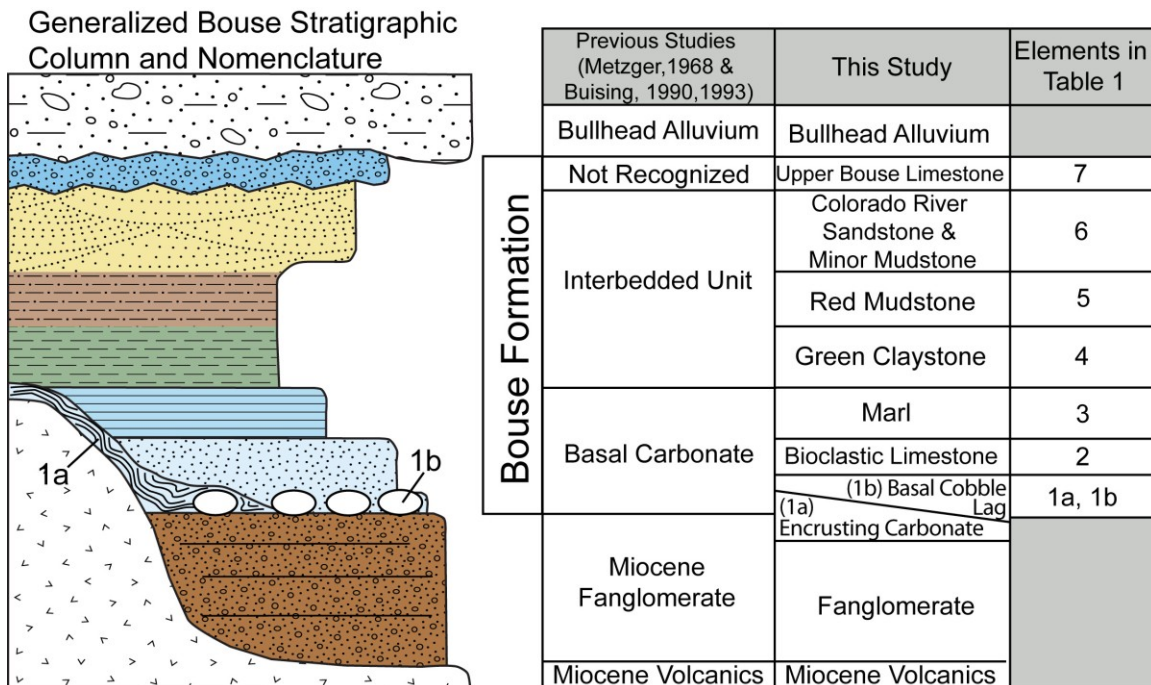
Figure 3. Generalized Bouse Formation stratigraphic column. Table includes Bouse units defined by previous studies as compared with units defined by this study.

9

further subdivide the same three intervals into six major facies. In addition, we add a 7th

facies (upper Bouse limestone) that was not recognized in previous studies (Fig. 3).

CHAPTER III

METHODS

Measured Sections

The primary method of data collection for this project consisted of measuring stratigraphic sections in exposures of the Bouse Formation in two areas (Fig. 2): Milpitas Wash and southeastern Palo Verde Mountains, California (Fig. 4), and the Cibola area of western Arizona (Fig. 5). All locations were documented with a hand-held GPS unit. Measurements for stratigraphic sections were made at the decimeter scale using a 1.5 meter Jacob staff. Measurement of sections was accompanied by detailed descriptions of sedimentary lithofacies, fauna, sedimentary structures, and stratigraphic position of photos and samples in each section (Appendix 1). In some areas it was necessary to traverse down a wash to move up section in the Bouse, because the gradient of the washes in these areas is less steep than the gentle dip of the Bouse Formation.

Construction of Stratigraphic Panels

We compiled data for lithofacies, thickness, and location of measured sections along a series of transects in the two study areas (Figs. 4 and Fig. 5) to construct detailed stratigraphic panels. We constructed two types of facies panels using two different methods. The first set of facies panels show the Bouse in their modern coordinates by placing each measured section at its present-day elevation, thus resembling highly detailed geologic cross sections with vertical exaggeration. The second set of stratigraphic panels were constructed by hanging the measured sections from a young, conformable contact that is used as a unique horizontal stratigraphic datum.

11
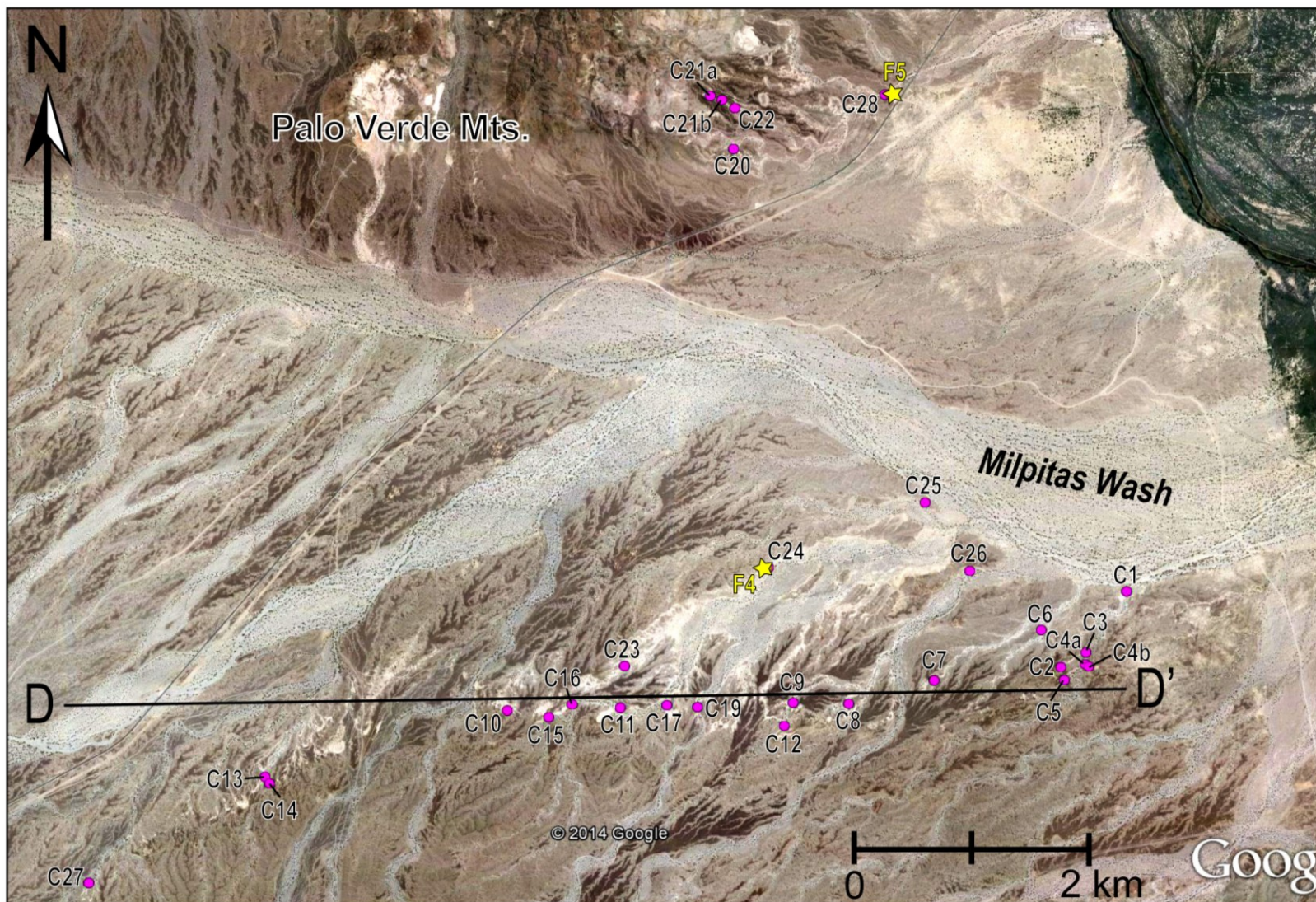
Figure 4. Milpitas Wash area, west of the Colorado River, California. Pink dots and numbers indicate location of measured sections. Yellow stars and numbers indicate location of faults that cut the Bouse. Black cross-section line indicates facies panel transect. This figure corresponds to inset locator box in Figure 2.
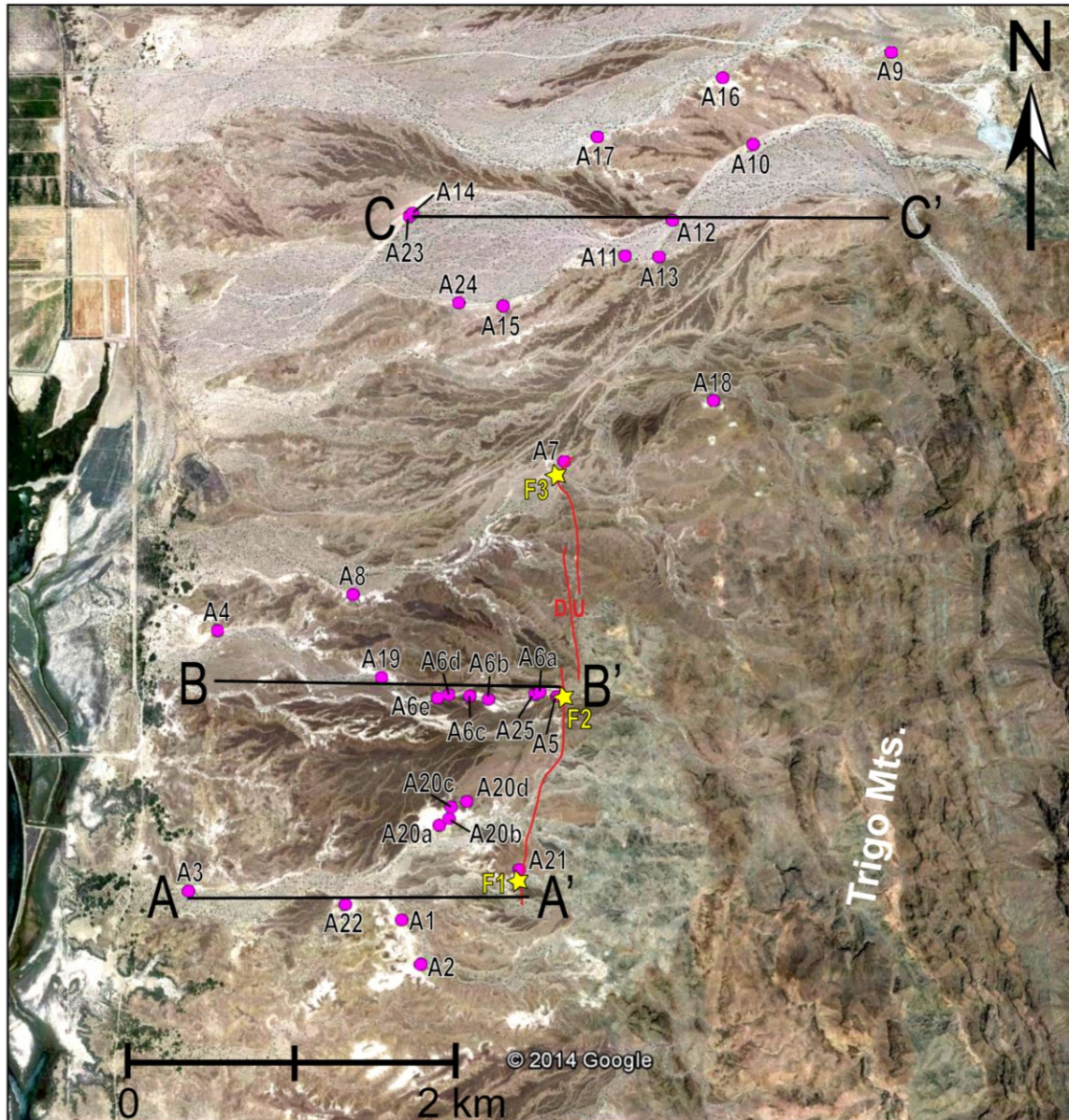
Figure 5. Cibola area, east of the Colorado River, Arizona. Pink dots and numbers indicate location of measured sections. Yellow stars and numbers indicate location of faults that cut the Bouse. Red lines indicate approximate locations of mapped faults. Black cross-section lines indicate facies panel transects. This figure corresponds to inset locator box in Figure 2.

Fault Analysis

Several faults that were found in the field to cut the Bouse were also analyzed.

Measurements, if possible, included strike and dip of the fault plane, plunge of any

striations, and dips of juxtaposed bedding. Again, all fault locations were documented and mapped with a hand-held GPS unit.

Thin Section Analysis and Sediment Accumulation Rates

A large number of hand samples were collected at various locations in the field and in measured sections, and were cut and made into thin-sections for further identification and analysis of sedimentary textures and fossils. Samples were selected for thin sections based on facies and faunal assemblages.

A number of varved marl samples were also collected at various locations in the field and within measured sections. Sediment accumulation rates were calculated by dividing a measured sample thickness by the number of varves or layers present in the sample in order to get a rate in mm/yr or m/ka. These samples were used to estimate and model sediment accumulation rates and therefore rates of duration for Bouse deposition. Accumulation rates were measured by assuming varves were annual and represented an entire year's worth of sediment deposition.

CHAPTER IV

RESULTS

Sedimentary Lithofacies

The southern Bouse Formation can be divided into seven major lithofacies, or

units, that include the basal carbonate of previous workers (units 1-3), interbedded unit

composed of Colorado River-derived siliciclastic sediment (units 4-6), and a previously

unrecognized upper limestone (unit 7) (Fig. 3). Each unit is identified on the basis of

unique lithology, grain size, texture, and sedimentary structures that preserve a record of

unique depositional processes and environments, as described in Table 1.

Unit 1 includes two subunits: basal encrusting carbonate, and basal cobble lag

(Table 1; Fig. 6). The basal encrusting carbonate consists of in-situ micritic boundstone

representing algal-stromatolitic mounds and tufa that grew in a shallow-water, near-shore

environment, coating local bedrock and locally the basal cobble lag. Basal cobble lag is a

uniquely concentrated layer of cobbles seen at the base of the bioclastic limestone that

was formed by reworking and winnowing of underlying alluvial fan sediments (Fig. 6).

Unit 2, bioclastic limestone, is composed of interbedded calcarenite, fossil shell hash, and

lithic sandstone and conglomerate that were transported and deposited in shallow-water,

near-shore to strandline environments by strong currents above wave base (Fig. 7). The

overlying marl, unit 3, consists of fine-grained micrite deposited in deep water below

wave base, with three facies variants that reflect presence or lack of thin laminations and

clay (Fig. 8). Green claystone, unit 4, is Colorado River-derived, siliciclastic clay

deposited by suspension settling in an offshore environment, below wave base (Fig. 9).

Unit 5, siliciclastic red mudstone, is massive to weakly bedded and contains common

Table 1. Description and Interpretation of Sedimentary Lithofacies in Bouse Formation.

| Lithofacies	Description	Interpretation
1a. Basal Encrusting Carbonate	Fig. 6A-D: Laminated micritic boundstone encrusting older rocks in concentric layers on underlying bedrock and conglomerate clasts. Commonly forms mounds.	Algal-stromatolitic mounds and coatings formed in near-shore, shallow water of lake or marine estuary.
1b. Basal Cobble Lag	Fig. 6D-F: Clasts concentrated at contact between Miocene fanglomerate and basal Bouse carbonate. Clasts mostly cobble size, range from pebble to small boulder; include volcanic, metamorphic, and plutonic rock. Clasts may be coated with encrusting algal carbonate or barnacles. Matrix is poorly sorted, coarse-grained, granular, lithic arenite sandstone, locally with bioclastic grains.	Reworking and winnowing of alluvial fan sediment by high-energy currents in lake or marine estuary. Matrix largely removed, leaving concentration of clasts. Local initial deposition of bioclastic carbonate.
2. Bioclastic Limestone	Fig. 7: Fine-to coarse-grained moderately to well sorted calcarenite and fossil hash mixed with variable % lithic sand, interbedded with well sorted lithic sandstone and conglomerate. Carbonate grains subrounded to well rounded shell fragments. Sedimentary structures include oscillatory and unidirectional ripple cross-lamination, trough cross-bedding, HCS, herringbone cross-bedding, ripple flaser bedding, planar stratification, and burrows. Fossils include barnacles, oncoids, ostracodes, gastropods, charophytes, clams, and algal coatings. Interbedded granule-pebble conglomerate dominantly siliciclastic with calcarenitic-lithic matrix and algal coated gravels. Abundant lateral interfingering and complex cross-bedding of bioclastic and siliciclastic facies.	Traction transport and deposition from migrating bedforms (ripples, dunes, sand waves, upper plane bed) by high energy currents in near-shore, shallow water, above wave base in a lake or marine estuary. Cross-bedded conglomerate records strong currents (unidirectional and oscillatory) in near-shore bars and beach ridges. Bioturbation structures produced by burrowing organisms (crustaceans?).
3. Marl	Fig. 8: Fine-grained micrite, occurs in 3 main variants: (1) internally structureless, massive white ~5-20 cm thick beds alternating with # 2 or 3; (2) mm-scale laminated micrite; and (3) yellowish fissile clayey micrite and amorphous silica in 20-40 cm thick beds. Ostracodes are common. Variants 1 and 2 are locally interbedded with calcarenite and concentrations of barnacles, oncoids, charophytes, clams, and/or gastropods.	Deposition by suspension settling of fine-grained carbonate in low-energy, off-shore, deep-water lake or marine estuary, below wave base. Up-section change from variants 1 & 2 to # 3 records initial weak input of Colorado River clay.
4. Green Claystone	Fig. 9A-C: Olive-green siliciclastic clay, weakly cemented, massive to weakly bedded, some ostracodes. Commonly interbedded with underlying yellow marl. Locally contains a distinct ~1 cm-thick bright orange rusty bed at the marl-claystone contact.	Deposition by suspension settling of Colorado-River clay in low-energy, off-shore lake or marine estuary. Rusty thin bed may be transported organic matter.

Table 1. (continued)

5. Red Mudstone	Fig. 9A, 9C-D: Red to orange siliciclastic mudstone and siltstone, massive to weakly bedded. Base of red mudstone is an abrupt contact with underlying green claystone. Locally contains interbedded calcarenite or green claystone, fist-sized mud geodes with large calcite crystals, and Colorado River sandstone. Where interbedded with cross-bedded Colorado River sandstone, red mudstone includes weakly developed paleosols with light tan, drab-haloed root traces and sand-filled desiccation cracks.	Low-energy deposition in shallow offshore to fluvial-deltaic floodplain (where paleosols and desiccation cracks present). Paleosols represent soils formed on floodplain adjacent to fluvial-deltaic channels of the first-arriving Colorado River.
6. Colorado-River Sandstone & Minor Mudstone	Fig. 10: Pink to tan, fine- to medium-grained, well sorted, quartz-rich sandstone with minor interbedded red mudstone. Sand grains are rounded to well rounded, pink-stained quartz with minor chert and lithic fragments. Thick multi-story cross-bedded sandstone is commonly channelized and eroded into red mudstone. Sedimentary structures include large scale trough cross-bedding (up to 3 m-thick x-bed sets), ripple cross-lamination, climbing ripples, horizontal stratification, and mudstone rip-up clasts.	Channels and floodplain of the first arriving Colorado River. Sand deposited by traction transport in large channels by migrating bedforms (dunes, sand waves, ripples). Minor muds are fluvial floodplain deposits. Rip-up clasts produced by erosion of underlying overbank mud during channel migration and avulsion events.
7. Upper Limestone	Fig. 11: Corse-grained calcarenite and calcarenite-matrix conglomerate with mixed carbonate and lithic sand-gravel (mainly locally derived). Carbonate grains dominantly abraded barnacles, green algae (*Codium*), and coralline red algae (*Sporolithon?*), plus minor oncoids, gastropods, ostracodes, bivalves, and charophytes. Conglomerate is moderately to poorly sorted with granule to cobble clasts in calcarenitic sandy matrix. Abundant horizontal and hummocky cross-stratification (HCS). Overlies and is locally interbedded with Colorado River Sandstone.	Unit records re-flooding of basin by standing body of water (lake or marine estuary). Deposition by high-energy near-shore currents, traction transport, migration of bedforms in shallow water above wave base. HCS produced by large storm waves and currents.

thin cross bedded sandstone beds, paleosols and mud cracks, which collectively record deposition in lake-margin mudflats of a river delta system (Fig. 9). Unit 6, Colorado River sandstone and minor muds, consists of thick-bedded, trough cross-bedded, multistory, channelized sandstone that commonly displays erosional relief cut into interbedded red mudstone (Fig. 10). We infer that this unit was deposited in channels

17
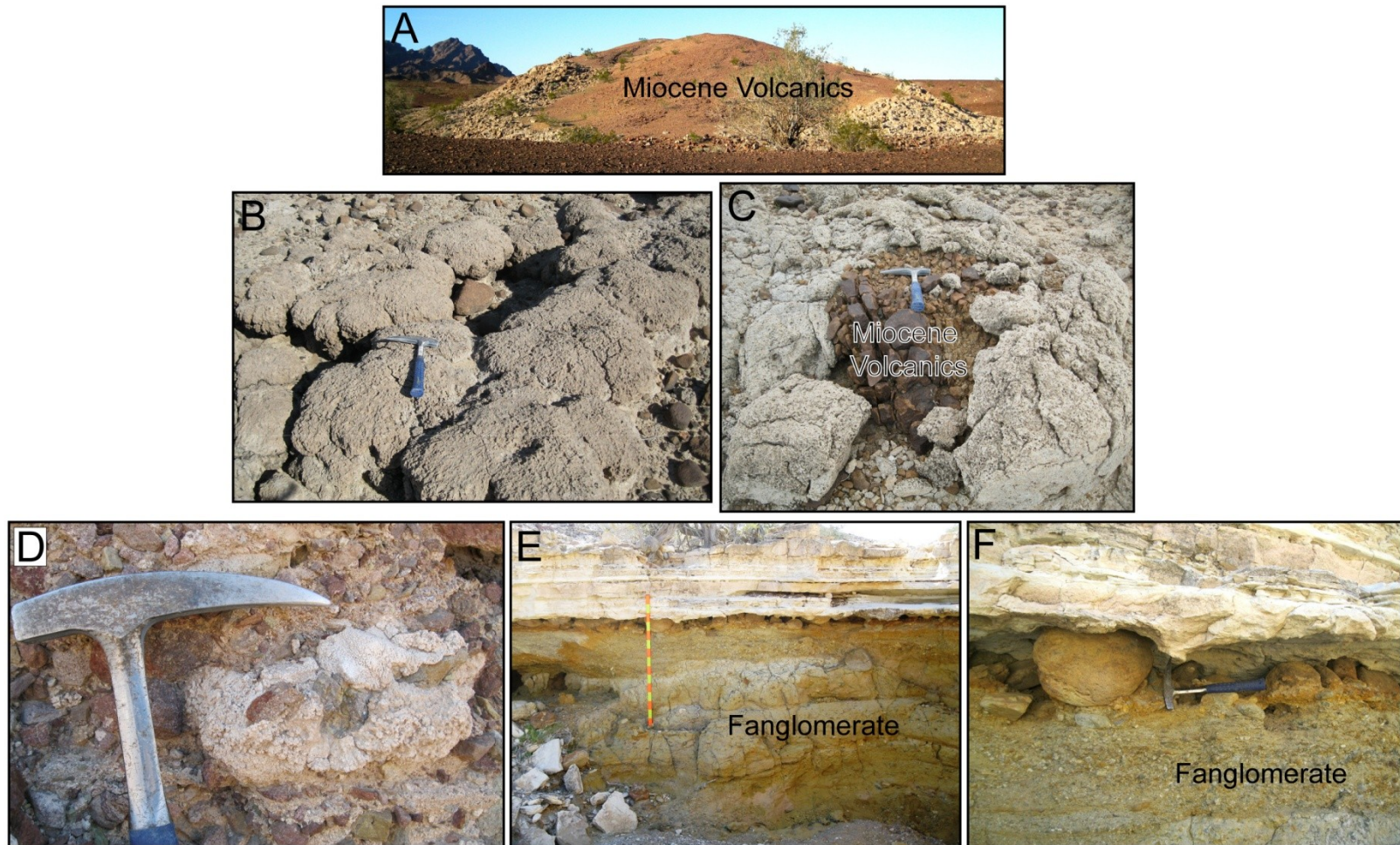
Figure 6. Photographs of encrusting basal carbonate (Unit 1a) and cobble lag (Unit 1b). (A) Small hill of encrusting basal carbonate draped on residual paleotopography of Miocene volcanic rocks. (B) Stromatolitic algal mounds of encrusting basal carbonate. (C) Weathered mound of encrusting basal carbonate with exposed Miocene volcanic boulder core. (D) Reworked upper part of fanglomerate with a clast of algal encrusting basal carbonate. (E) Upper ~2 m of fanglomerate with overlying basal cobble lag and lower ~1 m of bioclastic limestone. (F) Close-up of open-framework basal cobble lag with minor matrix.

18
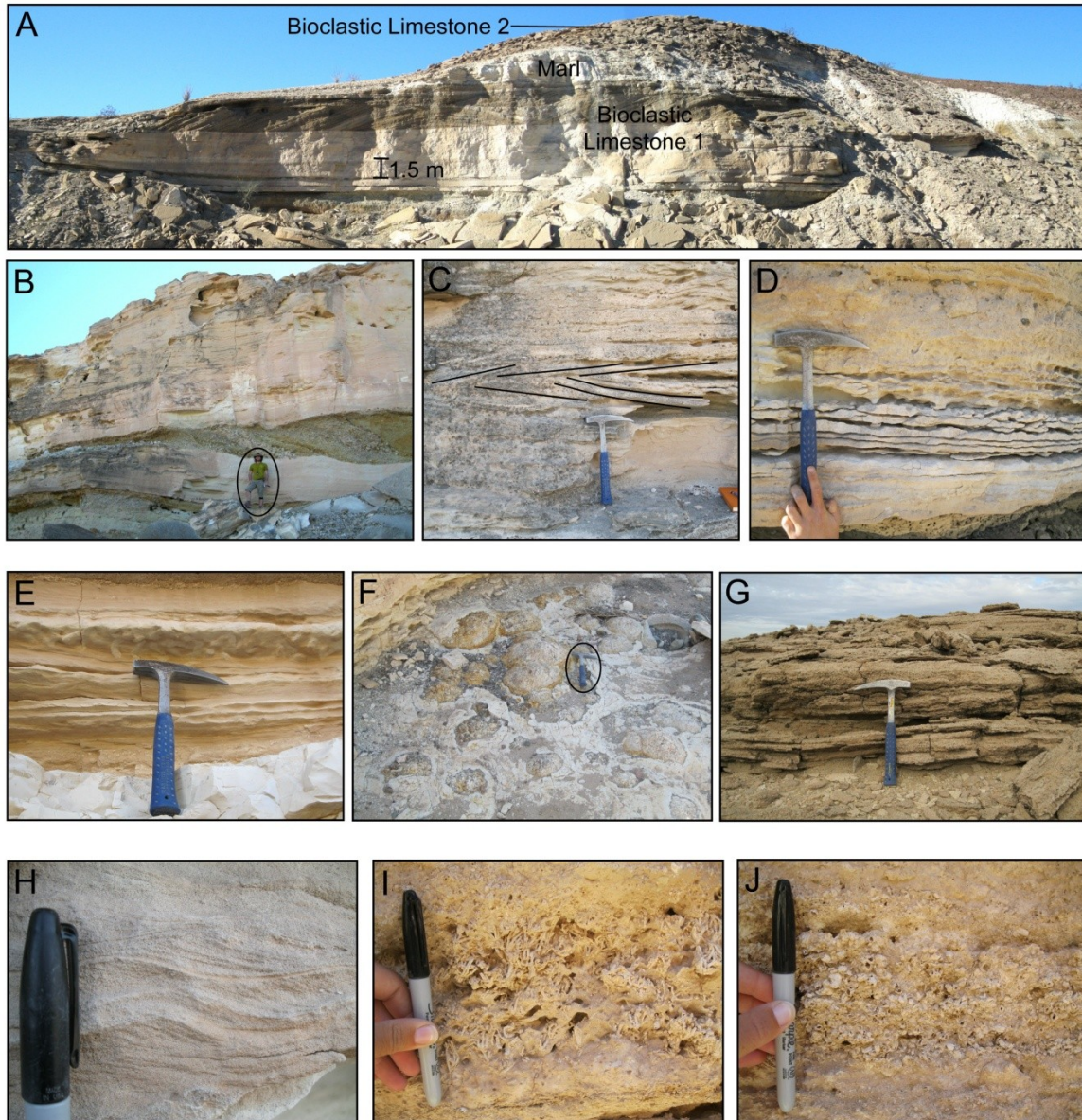
Figure 7. Photographs of bioclastic limestone (Unit 2). (A) Outcrop of interbedded and cross-bedded, bioclastic limestone, including fossil hash, calcarenite, conglomerate, and sandstone interbedded with marl. (B) Discontinuous lens of well sorted siliciclastic cross-bedded conglomerate in bioclastic limestone. (C) Herringbone cross-bedding in well sorted, medium-grained calcarenite. (D) Ripple flaser bedding in well sorted fine-grained calcarenite. (E) Burrows on underside of a calcarenite bed. (F) Algal-stromatolitc mounds on top of clasts of interbedded conglomerate unit. (G) Well sorted and horizontally stratified coarse grained barnacle-rich shell hash. (H) Climbing ripple cross-laminated, well sorted calcarenite. (I) Charophyte bed in bioclastic limestone. (J) Concentrated barnacle shell-hash bed in bioclastic limestone.

19
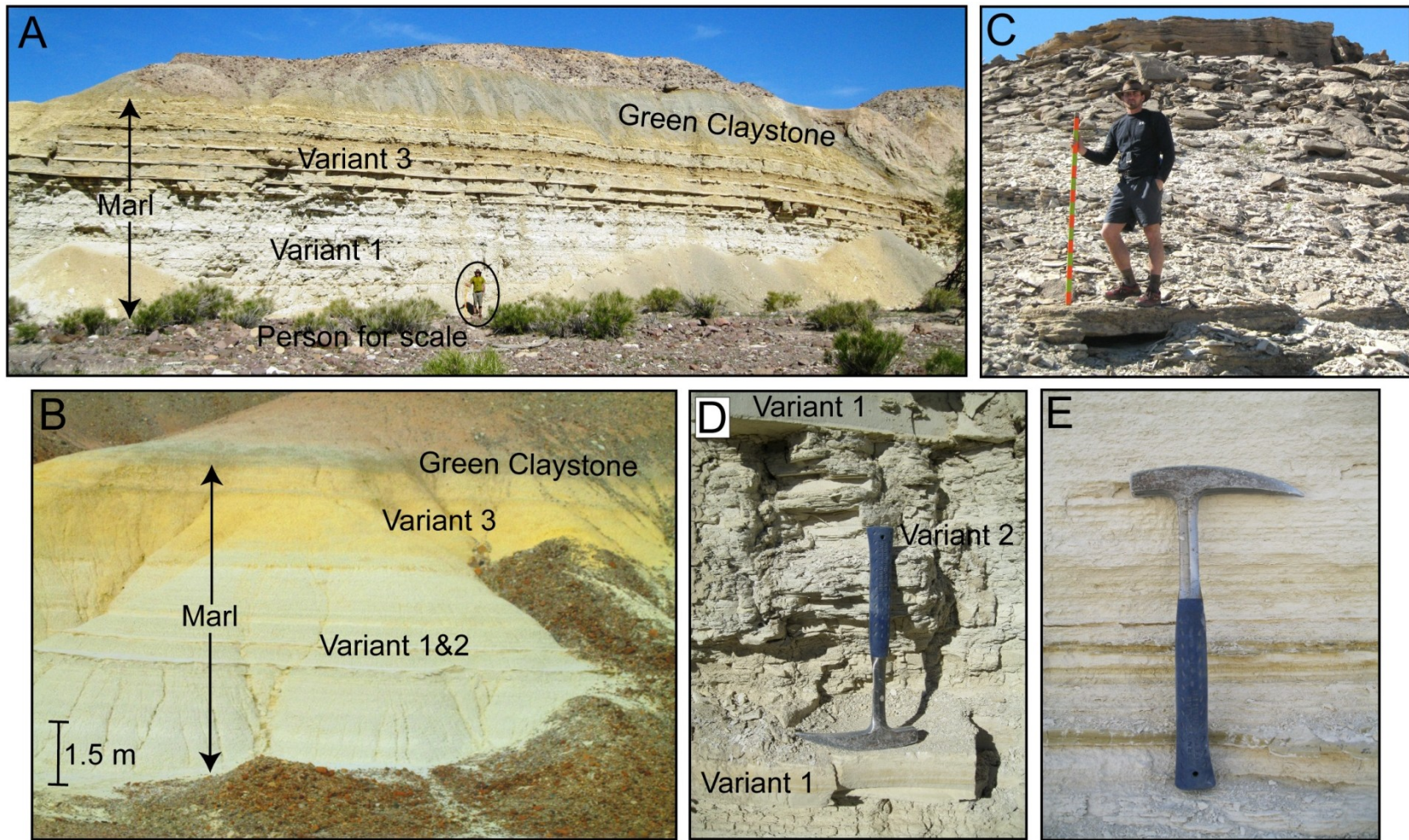
Figure 8. Photographs of marl (Unit 3). (A) Marl variants 1 (massive beds) and 3 (interbedded marl and clayey marl) with overlying green claystone. (B) Interbedded marl variants 1 and 2 (thinly laminated); overlain by variant 3 and green claystone. (C) Photo showing typical flaggy weathering style of thin bedded marl, variant 1. (D) 50 cm interval of thinly laminated variant 2 marl, micritic shale, between two 10 cm beds of massive variant 1 marl. (E) Thinly interbedded and stratified marl and calcarenite.
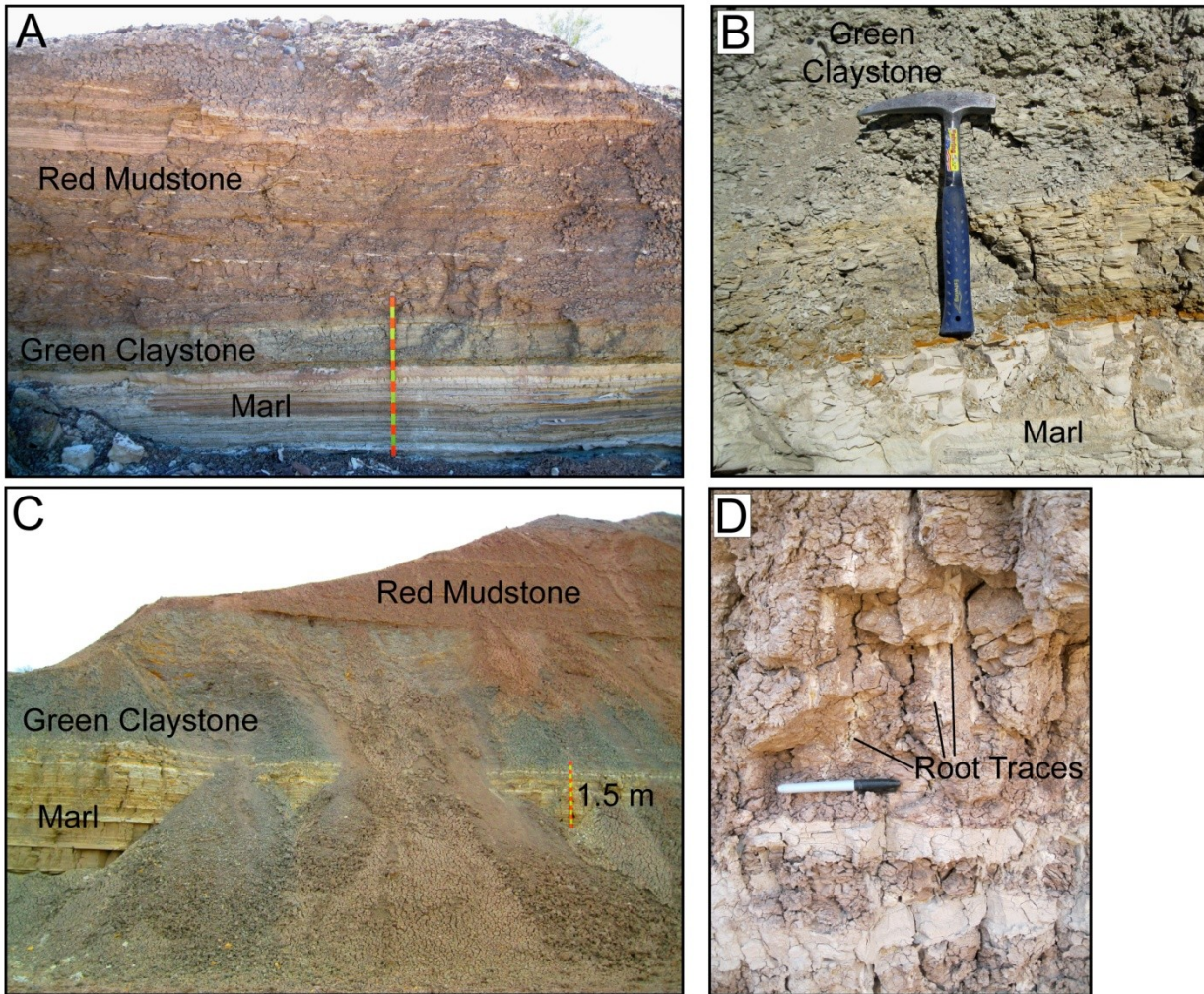
Figure 9. Photographs of green claystone (Unit 4) and red mudstone (Unit 5). (A) Outcrop of marl overlain by thin green claystone and thicker red mudstone units. (B) Contact between marl and green claystone with characteristic 1 cm thick bright orange rust bed. (C) Outcrop of marl overlain by green claystone and red mudstone. (D) Red mudstone paleosol with drab-haloed root traces, mud cracks, and minor interbedded Colorado River sandstone.
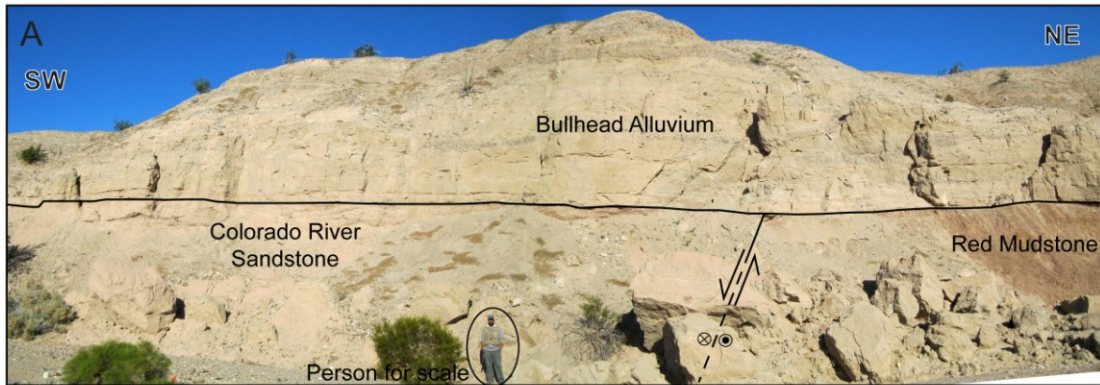
Figure 10. Photographs of Colorado River sandstone and mudstone (Unit 6). (A) Outcrop of Colorado River sandstone juxtaposed against red mudstone by an oblique dextral-normal fault that pre-dates deposition of the Bullhead Alluvium. Most of the fault is covered, but it is well exposed just beneath the contact with Bullhead. (B) Outcrop of multistory thick-bedded trough cross-bedded Colorado River sandstone and minor mudstone, capped by Quaternary terrace gravel. (C) Close-up of outcrop in B showing cross-bed foresets with small scale internal climbing-ripple cross-lamination.

and adjacent floodplains of the Colorado River when it first flowed through to the Gulf of California, as discussed in more detail below. Unit seven, upper limestone, consists of sandy calcarenite and calcarenite-matrix conglomerate interbedded locally with Colorado River sediment and erosionally inset into underlying units 3-6 (Fig. 11). This unit records re-flooding of the basin by a standing body of water (lake or marine estuary) after first arrival of the Colorado River and its sandy sediment load.

Stratigraphic Architecture

Cibola, Arizona

Three east-west facies panels in the Cibola, Arizona, area (Fig. 5) depict stratigraphic architecture of the Bouse Formation in modern and restored coordinates for each transect. The southernmost facies panel, A-A' (Fig. 12), reveals several important features in both the modern and restored panels. Interbedded bioclastic limestone and marl units display some thickness variations including pinching-out of marl 1, and bioclastic limestone 1 roughly doubles in thickness from ~7 m in the east to ~14 m in the west. A normal fault in the east has at least 20 m of vertical throw, and juxtaposes Bouse basal carbonate against older Miocene fanglomerate. This transect contains very little green claystone and overlying Colorado River sediment, which mostly has been eroded away and replaced by Quaternary terrace gravel (QTG). The restored panel (Fig. 12B) reveals overall subhorizontal primary bedding dips and little evidence for syn-depositional tilting, in contrast to the middle and north Cibola facies panels.

The middle facies panel in the Cibola area, B-B', reveals westward thickening of the basal carbonate from less than 10 m in the east to over 30 m in the west (including thicknesses projected into the subsurface (Fig. 13). Pronounced westward thickening is

23
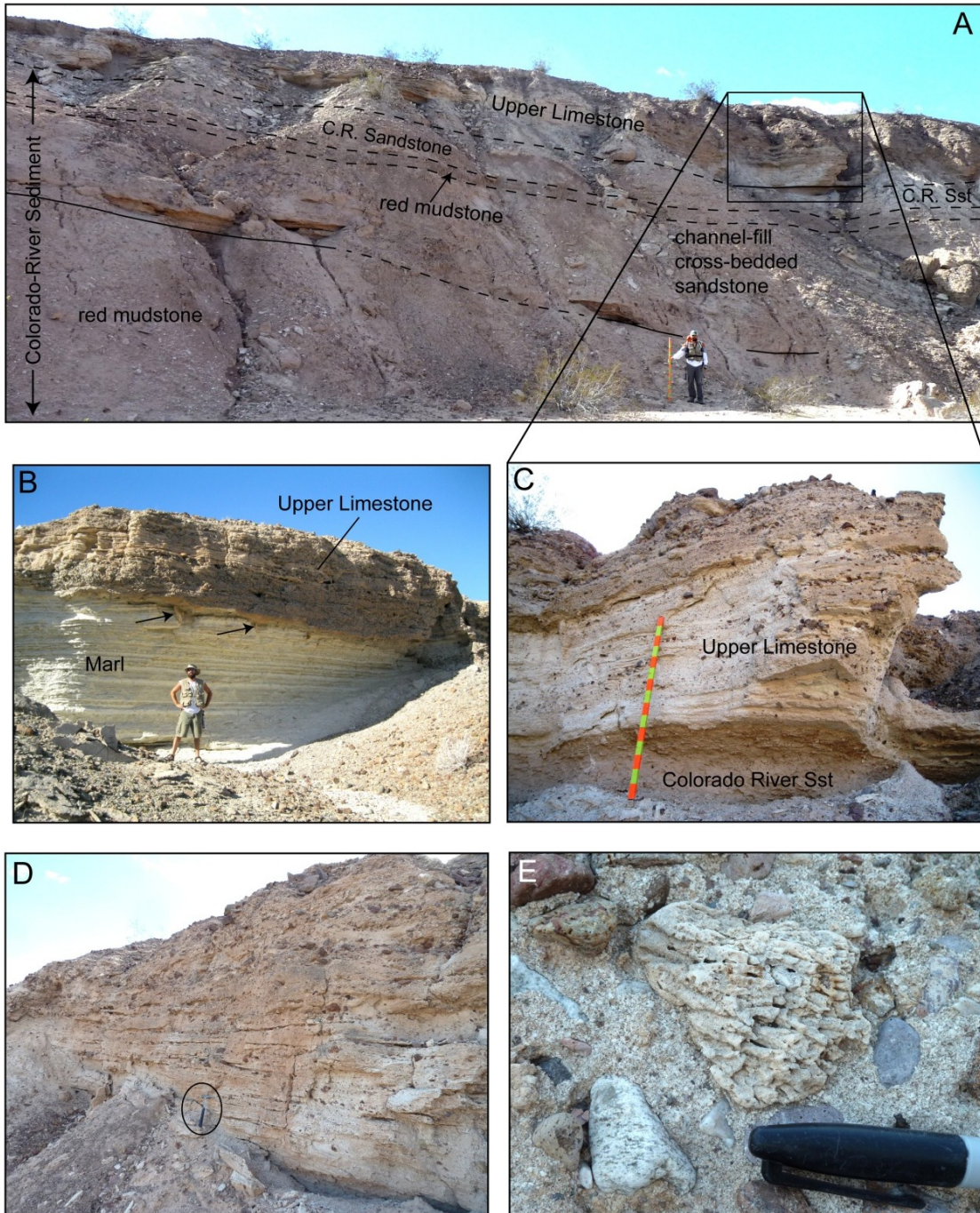
Figure 11. Photographs of upper limestone (Unit 7). (A) Outcrop of thick channelized cross-bedded Colorado River sandstone overlain by upper limestone. (B) Outcrop of marl erosionally overlain by upper limestone; arrows point to desiccation cracks in marl. (C) Close-up of outcrop in A, showing base of upper limestone where it directly overlies Colorado River sandstone. (D) Upper limestone unit showing well developed horizontal to low-angle cross stratification, and hummocky cross-stratification (HCS). Hammer (circled) for scale is 32.5 cm long. (E) Close-up of reworked branching green algae *Codium*, commonly found in upper limestone unit, surrounded by sandy calcarenite-matrix conglomerate.

24
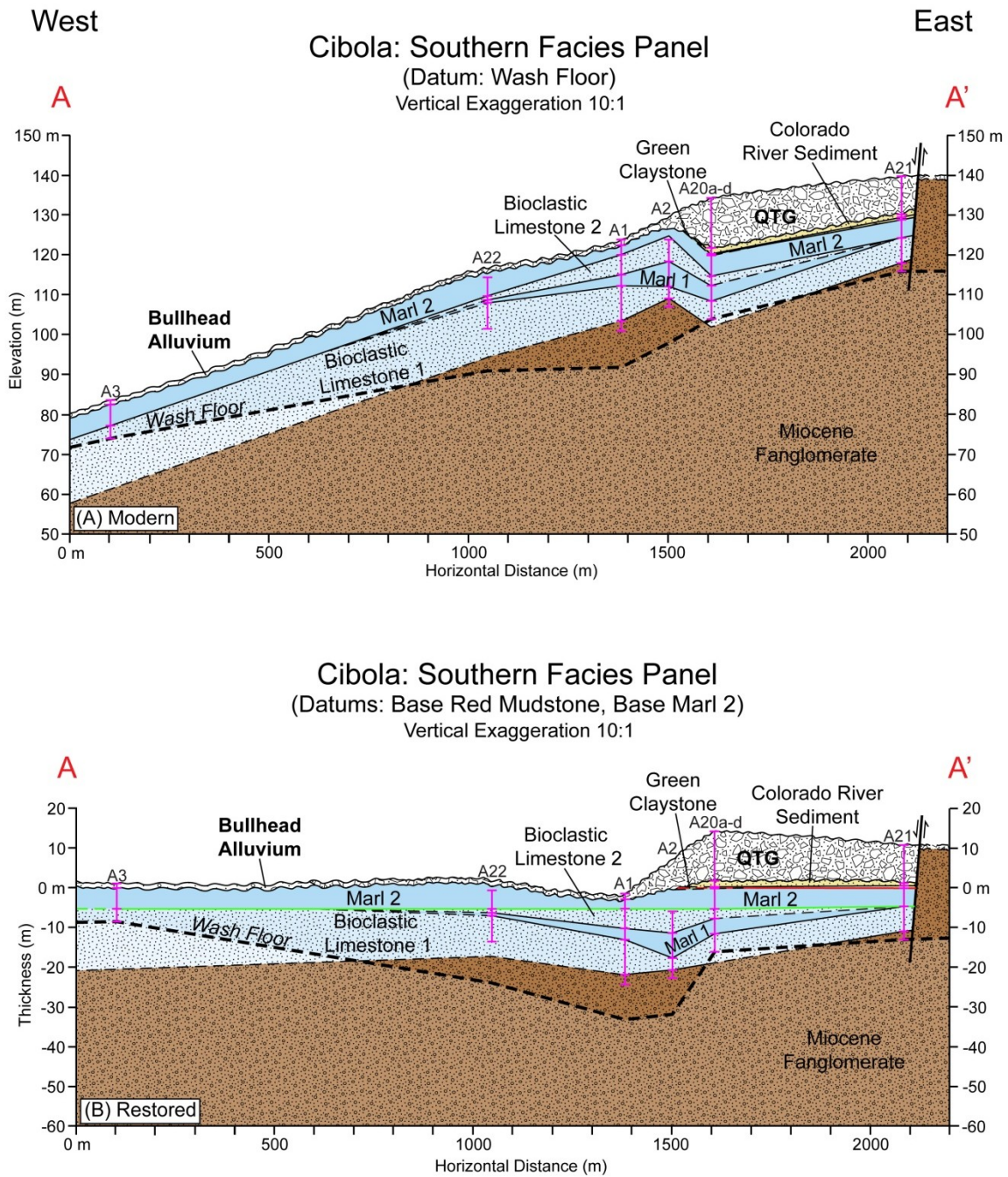
Figure 12. Facies panels constructed along southern transect A-A' in Cibola, AZ area (location in Fig. 5). (A) Facies panel plotted in modern coordinates (elevation and distance), with sections placed vertically based on height above wash floor. (B) Restored facies panel hung from two stratigraphic datums: base of the red mudstone and base of marl 2.
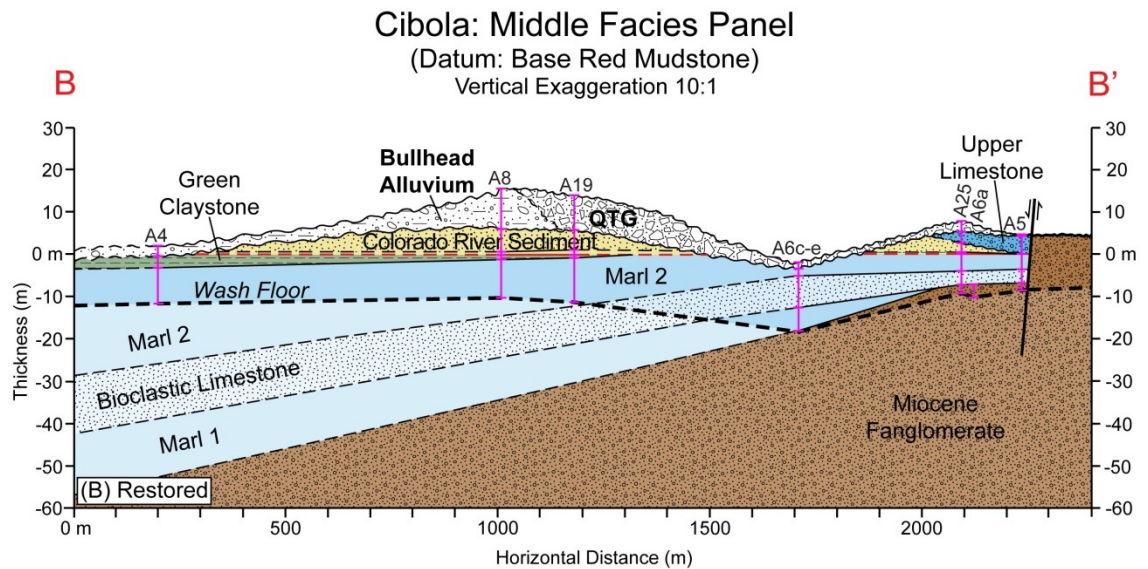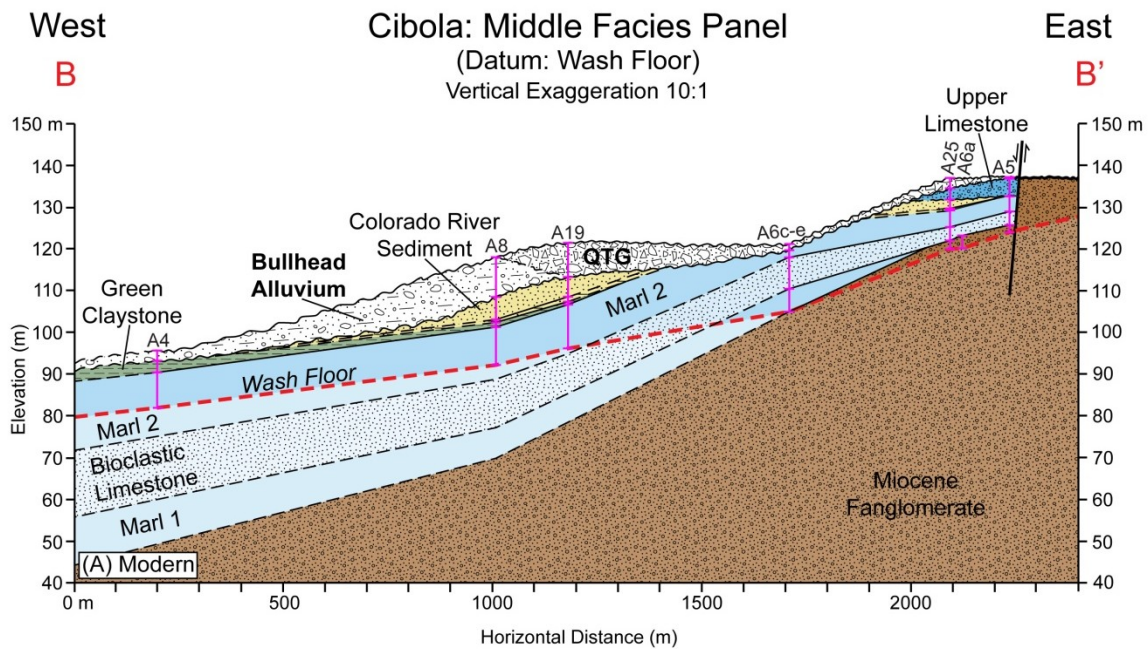
Figure 13. Facies panels constructed along middle transect: B-B' in Cibola, AZ area (location in Fig. 5). (A) Facies panel plotted in modern coordinates (elevation and distance), with sections placed vertically based on height above wash floor. (B) Restored facies panel, hung from the base of the red mudstone.

accompanied by lateral pinch-out and truncation of marl 1 and green claystone to the

east. The same normal fault seen in facies panel A-A' cuts the Bouse Formation near the

26

east end of this panel, with a vertical throw of at least ~12 m. This transect preserves

more of the green claystone and Colorado River sediment than panel A-A', and includes

an important interval of upper limestone that erosionally overlies and is inset into

Colorado River sandstone, green claystone and marl 2 near the normal fault (Fig. 13).

Large sand-filled, 20- to 50-cm deep desiccation cracks are present in the marl 2 unit

directly beneath its erosional contact with the upper limestone (similar to Fig.11B).

Additionally, section A25 shows local interbedding of Colorado River sediment in the

upper limestone unit. The westward stratal thickening and wedge geometry seen in this

panel, when plotted in restored coordinates (Fig. 13B), require a gentle primary bedding

dip to the west that suggests subtle syn-depositional tilting prior to deposition of

Colorado River sandstone and red mudstone.

Facies panel C-C' (Fig. 14) also reveals westward thickening of the basal

carbonate units and lateral pinchout of marl 1 to the east. The normal fault seen in the

first two panels is not present at this latitude, and instead a subtle monoclinal fold hinge

is revealed in the restored coordinates (Fig. 14B), with a horizontal eastern limb indicated

by the laterally continuous thin bioclastic limestone unit. The western part of this facies

panel contains much thicker green claystone and cross-bedded Colorado River sandstone

(e.g. Fig. 10) compared to thicknesses seen in panels A-A' and B-B'. Comparison of the

modern and restored facies panels reveals the influence of post-depositional deformation

and uplift in the western part of panel C-C' (Fig. 14).

Milpitas Wash, California

One stratigraphic facies panel (Fig. 15) was constructed along an East-West

transect for the Milpitas Wash, California, area (Fig. 4). This panel is hung from the base

of marl 2 and depicts the restored Bouse architecture during time of deposition. It shows
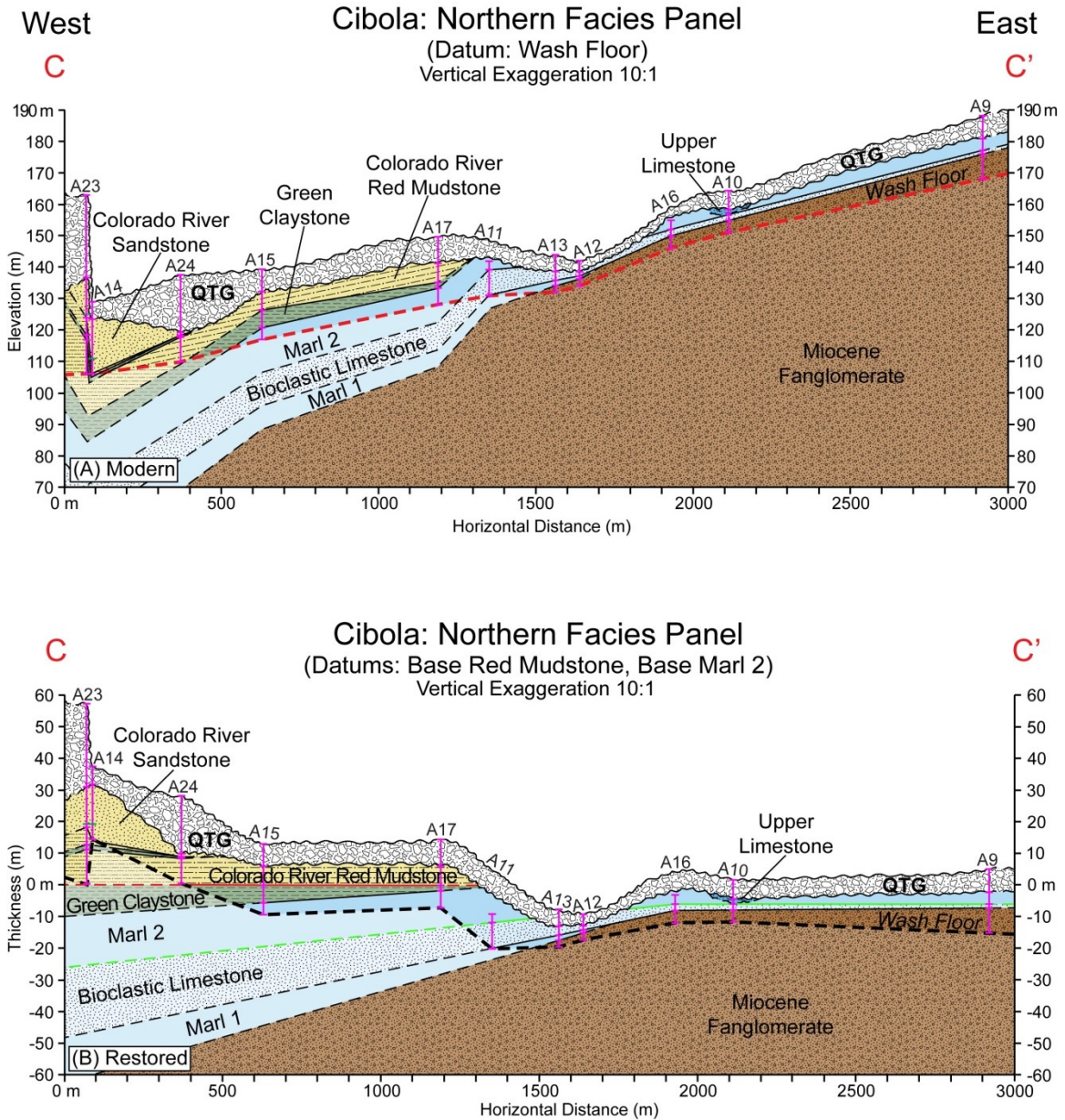
Figure 14. Facies panels constructed along northern transect: C-C' in Cibola, AZ area (location in Fig. 5). (A) Facies panel plotted in modern coordinates (elevation and distance), with sections placed vertically based on height above wash floor. (B) Restored facies panel hung from two stratigraphic datums: base of the red mudstone and base of marl 2.

interbedding and lateral interfingering of the bioclastic and marl units. Green claystone

and Colorado River sediment here are overlain by Bullhead Alluvium, which is overlain

by QTG. At about 5500 m in this transect a northwest striking dextral normal fault

juxtaposes Colorado River sandstone against older red mudstone (Fig. 10A). The upper
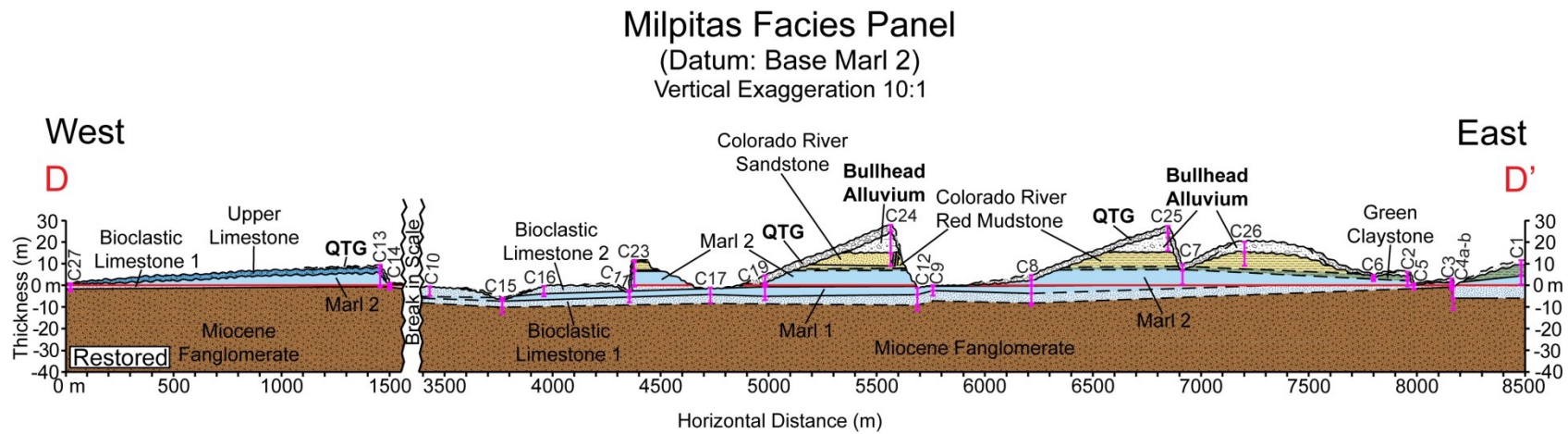
Figure 15. Restored facies panels constructed along transect: D-D' in Milpitas Wash, CA area (location in Fig. 4). Datum used for construction is the base of marl 2.

limestone unit in the Milpitas area is present only in outcrops to the west, where it is erosionally inset into the underlying marl unit (Fig. 11B).

Southeast Palo Verde Mountains, California

For the southeastern Palo Verde Mountains area (Fig. 4) the Bouse Formation is represented in a composite section that was constructed by correlating three measured sections (C20, C21a&b, and C22) using a distinct, laterally extensive calcarenite bed (Fig. 16). The composite section displays a vertical stratigraphic succession similar to that seen in the other study areas. Miocene fanglomerate is overlain by the basal carbonate (bioclastic and marl units), which is overlain by green claystone and red mudstone. The red mudstone thickens dramatically to the east from measured section 21 to 22, and the upper limestone unit erosionally overlies a thick interval of cross-bedded Colorado River channel sandstone (Figs. 11, 16).

Summary and Interpretation of Stratigraphic Relations

The southern Bouse Formation in the study area displays systematic facies relationships and stratal geometries that are important for interpreting controls on basin evolution and first arrival of Colorado River sediments. The lower bioclastic limestone is in most places the oldest carbonate unit and rests directly on the cobble lag (where present) at the top of Miocene fanglomerate. The marl and bioclastic units tend to be interbedded and commonly exhibit lateral interfingering with each other, but marl is always the youngest carbonate unit, and it is directly overlain by the green claystone along a gradationally abrupt conformable contact. The green claystone is a widespread, laterally continuous, thin unit that pinches out toward the eastern and western margins of

30
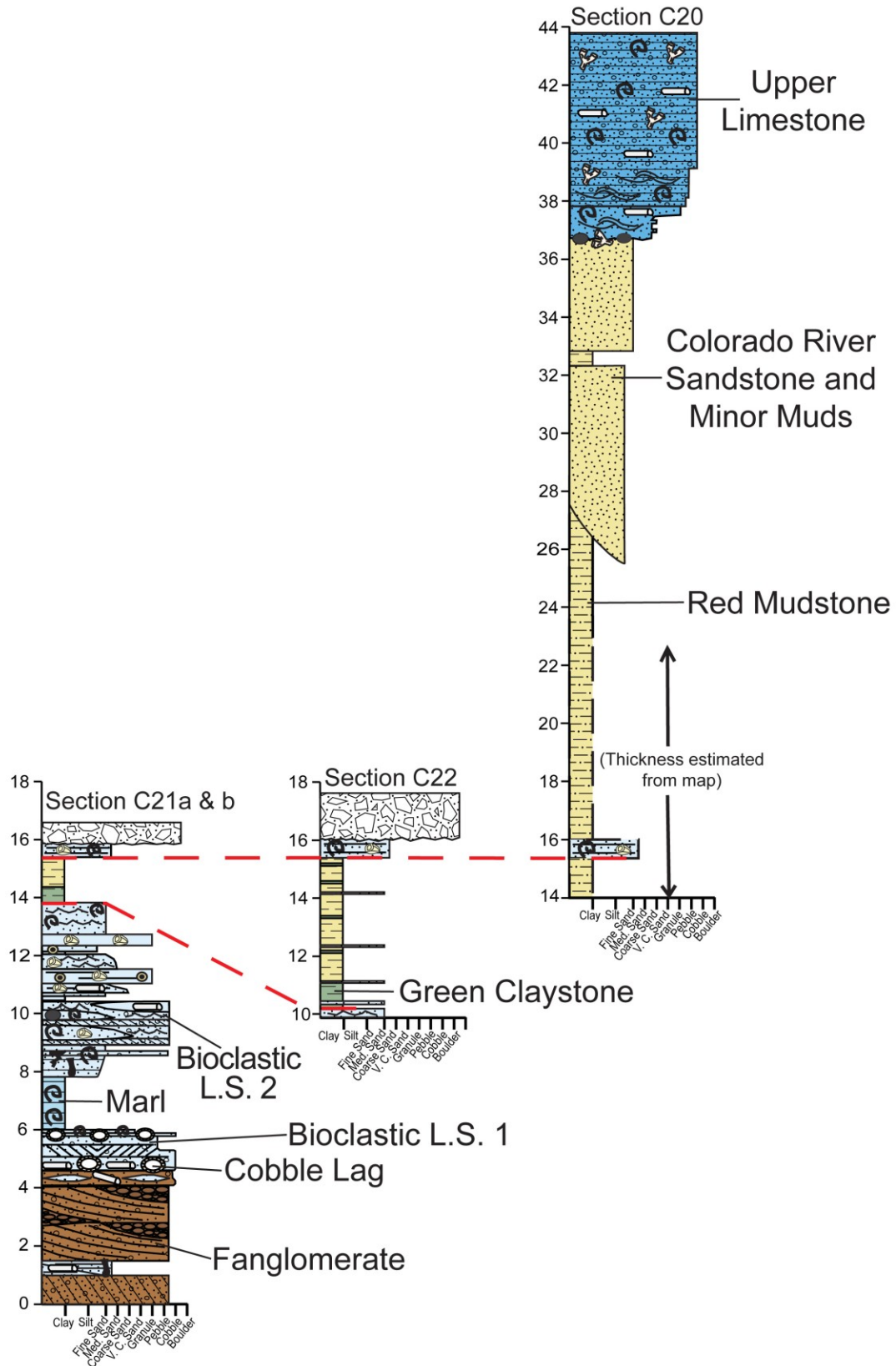
Figure 16. Composite measured section from the southeast Palo Verde Mountains (location in Fig. 4).

31

the Bouse depocenter, where the younger red mudstone rests directly on marl. Thick, channelized cross-bedded Colorado River sandstone is interbedded with red mudstone that contains distinctive paleosols and mud cracks; together they record the earliest establishment of a through-going Colorado River in this region.

The upper limestone unit is younger than and erosionally inset into Colorado River channel sandstone, red mudstone, and locally the youngest marl unit. Where the upper limestone rests directly on marl, the marl contains 20- to 50-cm deep sand-filled desiccation cracks that require significant lowering of base level because the marl accumulated offshore below wave base (though water depth is not well known).

The combination of systematic westward thickening, stratal wedge geometries, and eastward pinch-out of units in the Cibola area (Figs. 13B, 14B) represents a unique stratigraphic architecture not recognized in previous studies of the Bouse Formation. These geometries reveal a gentle dip toward the basin center that existed prior to deposition of upper Bouse Colorado River sandstone. Basinward dips likely formed either by (1) deposition of carbonate on a pre-existing inclined surface representing the side of an older inherited valley ("mega-drape" of House et al., 2005), or (2) by subtle syn-depositional tilting toward the basin center beneath the modern Colorado River, or possibly a combination of these mechanisms. Post-depositional deformation is clearly recorded in areas where the Bouse is cut by normal faults (Figs. 12, 13) or displays local bedding dips steeper than 10° that likely can't be explained by draping of deposits onto pre-existing valley paleotopography. The implications of these observations for regional tectonics and evolution of the Colorado River are discussed below.

32

Post-Bouse Faults

Three major faults or fault systems were identified in this study: (1) one normal fault system southeast of Cibola in Arizona for which we investigated three localities, labeled F1-F3 on Fig. 5; (2) one fault near Milpitas Wash, CA, labeled F4 (Fig. 4); and (3) one fault in the SE Palo Verde Mountains, CA, labeled F5 (Fig. 4).

The steep normal fault system identified near Cibola was observed in outcrop in three different localities (Fig. 5). However, only in one locality (Fig. 17A) was the fault plane exposed well enough to measure, where it strikes ~north and dips 58˚ W. This fault can be seen in the southern and middle facies panels (Figs. 12, 13), where it drops younger Bouse sediment down against older Miocene fanglomerate.

The fault identified in Milpitas wash (Fig. 10A, 17B) strikes 137˚ and dips 71˚ W. Striations measured on the fault plane have a plunge of 63˚SE, indicating that the fault had oblique, dextral-normal sense of slip. Bedding in a drag fold ~50 cm east of the fault (Fig. 17B) has a strike of 170˚ and dip of 49˚ W. This fault juxtaposes older Colorado River sandstone against younger red mudstone, and the entire interval is capped erosively by Bullhead Alluvium (Fig. 10A).

The last fault, observed in the SE Palo Verde Mountains (Figs. 4, 17C), has a fault plane strike of 322˚ and a dip of 83˚ NE. A zone of scaly fabric ~40-50 cm wide has striations with a plunge of 5˚NW in the fault plane. This large, nearly vertical fault within the red mudstone exhibits vertical bedding on either side of the fault (Fig. 17C). The kinematics of this fault are not well understood, although horizontal striations and steep bedding dips adjacent to the fault suggest it may be a large strike-slip fault. The faulted interval here is capped by either the Bouse upper limestone or QTG.
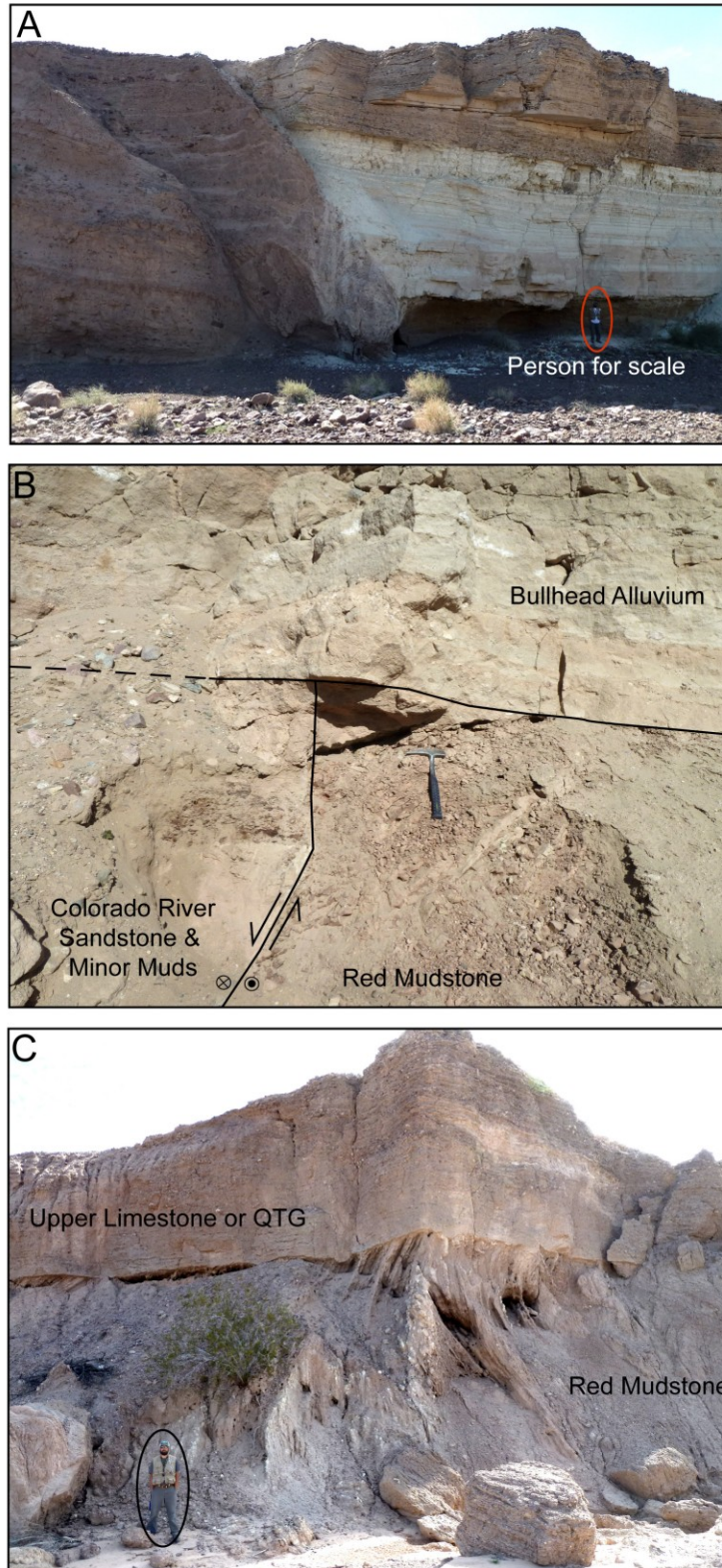
Figure 17. Faults that cut the Bouse. (A) View looking ~south at steeply west-dipping normal fault near Cibola, AZ. (B) Close-up view looking ~NW at oblique, dextral-normal fault near Milpitas Wash, CA (Figs. 4, 10A). (C) View looking ~SE at sub-vertical fault in SE Palo Verde Mountain area (Fig. 4).
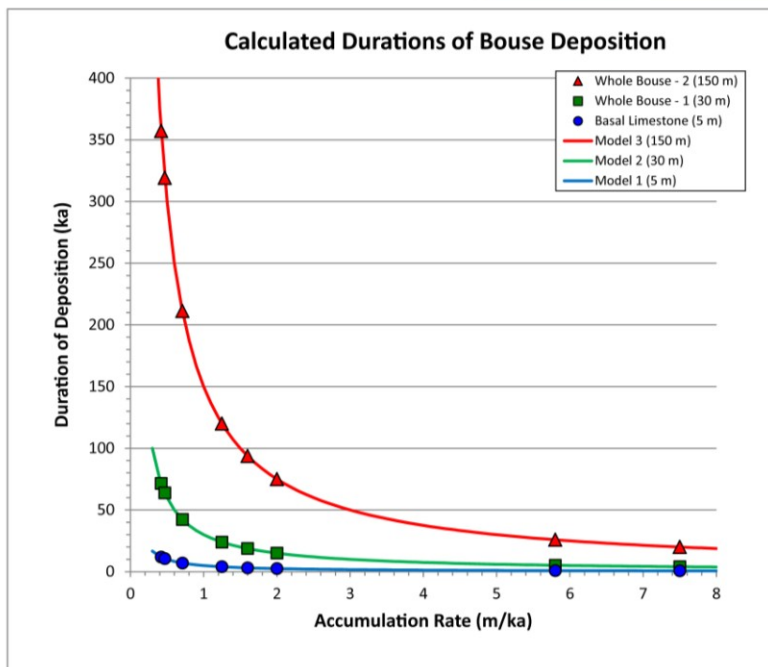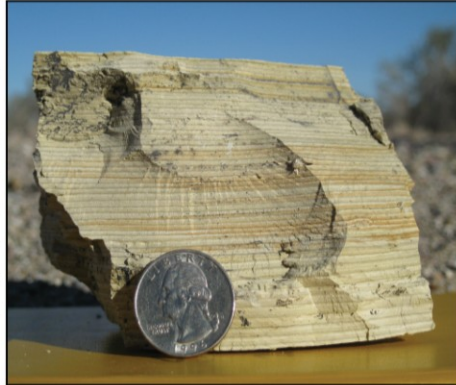
Sediment Accumulation Rates

Eight samples of varved marl were collected, and varves (assumed to be annual) were measured in order to estimate a range of possible sediment accumulation rates and total durations for the Bouse Formation (Fig. 18). Calculated sediment-accumulation rates range from 0.42 to 7.5 mm/yr, with most of the values clustered between 0.42 and 2.0 mm/yr. Based on these rates, we use a range of thicknesses for the Bouse Formation to calculate an estimated duration of Bouse deposition. The first thickness, representing only the basal Bouse Limestone (~5 m), predicts a very short duration (0-17 ka.) for deposition of the Bouse. If we use an average thickness of the entire Bouse exposed in outcrop in the southern paleolake Blythe area (~30 m), the predicted duration of deposition is a bit longer, ranging from 4-100 ka. The greatest thickness used in these calculations, 150 m, is an average of the total Bouse thickness measured from subsurface data in the paleolake Blythe area (Metzger, 1968; Metzger et al., 1973), and predicts the longest duration of deposition ranging from 19 ka to over 350 ka (Fig. 18).

Despite the large range of calculated sediment accumulation rates measured for the Bouse, the majority of the samples appear to cluster around ~1-2 m/ka, suggesting that the total thickness of the Bouse may have accumulated over roughly 50 to 350 ka. Previous studies have proposed that the Blythe paleolake existed for ~20-40 ka and that this provided sufficient time to create a saline lake with salinities high enough to support marine fauna that became well established and persisted in the fossil record (Spencer et al., 2008; Spencer et al., 2013). Data presented here suggest that, if we use the entire Bouse thickness documented from the subsurface beneath the Colorado River floodplain (Metzger et al., 1973), the calculated duration of deposition suggests a longer-lived

paleolake Blythe, possibly 300-400 ka. Of course accumulation rates calculated for the

marl do not necessarily apply to other units with different sedimentology, so this analysis

is presented mainly to stimulate discussion of this interesting question.

Sample #	Section #	Thickness(mm)/ #Layers	Rate (mm/yr) & (m/ka)
HB13-4	C-1	35.0/22	1.6
HB13-6	C-1	10.0/14	0.71
HB13-14	C-7	10.0/21	0.47
HB13-18	C-9	10.0/8	1.25
HB13-66	A-4	35.0/6	5.8
HB14-4	N/A	5.0/12	0.42
A15a	A15	60.0/8	7.5
A15b	A15	20.0/10	2.0

Figure 18. Image shows example of marl with annual varves, counted and used to calculate sediment accumulation rates as seen in the table. Graph shows different models for duration of Bouse deposition depending on thickness of Bouse used and range of sediment accumulation rates determined from measurement of varves.

36

CHAPTER V

DISCUSSION

The depositional history of the Bouse Formation is highly controversial, specifically with regard to two problems: (1) the environment of deposition in the southern paleo-lake Blythe; and (2) the age and duration of Bouse deposition. Contrasting interpretations from previous studies conclude that the Bouse was deposited in a marginal-marine estuary or series of inland lakes, or possibly a hybrid lake-estuary system (Metzger, 1968; Winterer, 1975; Buising, 1988, 1990; Spencer and Patchett, 1997; Spencer et al., 2008; Roskowski et al., 2010; Dorsey et al., 2013). In addition, the first arrival of Colorado River sand in the Salton Trough has been dated at 5.3 Ma, providing evidence for a through-going Colorado River by that time (Dorsey et al., 2007, 2011). However, this is complicated by the presence of the 4.8-Ma Lawlor Tuff interbedded in the southern Bouse Formation (Sarna-Wojcicki et al., 2011; Harvey, 2014). Prevailing conceptual models assume that the river did not become established until after the end of Bouse deposition, suggesting that the first arrival of a through-going river should be younger than 4.8 Ma (e.g., Spencer et al., 2013). Aspects of both controversies are addressed below, with interpretations of Bouse sequence stratigraphy and associated implications for regional tectonics.

Depositional Environments

Determining whether the Bouse Formation was deposited in a lake or marine estuary has been a fundamental challenge in assigning a primary environment of deposition to the Bouse. The Bouse contains a rather abundant list of marine fossils, including: (1) marine planktic and benthic foraminifers such as *Bolivina subexcavata* and

Globigerina sp. (Smith, 1970; McDougall, 2008; McDougall and Miranda-Martinez, 2014); (2) the fossil fish *Colpichthys regis*, known from shallow marine and brackish environments in the Gulf of California (Todd, 1976); (3) the intertidal gastropod *Batillaria californica*, whose closest relative is found in the Gulf of Mexico and Caribbean Sea (Taylor, 1983); (4) ostracodes *Cyprideis castus* and *Perrisocytheridea*, which live in the Gulf of California and coastal Baja California (Sandberg, 1966); and (5) newly recognized calcareous red algae *Sporolithon*, green algae *Codium*, and echinoderm *Astrodapsis* (pers. comm., Greg Retallack; Dorsey et al., 2013).

The Bouse Formation also displays abundant facies and sedimentary structures typical of tidally influenced marginal-marine environments such as bioturbation, hummocky cross-stratification, ripple-flaser bedding, and herringbone cross-bedding as shown previously in Figures 6-9. Despite the abundant evidence for a marine-estuary environment of deposition, Sr-isotope studies of the Bouse Formation (Spencer and Patchett, 1997; Spencer et al., 2008; Roskowski et al., 2010) reveal $^{87}Sr{:}^{86}Sr$ ratios that are similar to modern Colorado River water, not modern marine water. The new data presented here do not directly resolve the controversy over the Bouse depositional environment. Recent studies by Bright et al. (2014) and McDougall & Miranda-Martinez (2014) present new data from micropaleontology and stable isotopes that suggest a possible shift from lagoonal and inner neritic marine estuary to saline lake at the transition from green claystone to marl (Fig 8, 9). This contact is stratigraphically unique, distinctive, and laterally correlative, recording a pronounced shift from deposition of carbonate micrite to Colorado River derived siliciclastic clay. New results from micropaleontology and isotope geochemistry suggest that this change in lithology

may record a fundamental change in water composition and environment that resulted from a sudden large increase in water discharge from the newly arriving Colorado River (McDougall and Miranda-Martinez, 2014; Bright et al., 2014).

Even without knowing the exact environment of deposition, the stratigraphic changes in lithologies and fossils in the Bouse Formation provide excellent insight into changes in current energy and relative water depth through time. The stratigraphically lowest units, including cobble lag and bioclastic limestone, record deposition by high-energy currents in shallow-water to strandline and beach environments above wave base. The bioclastic limestone is overlain by fine-grained marl in a widespread up-section change that records transition to a lower energy environment in which micrite accumulated in standing water below wave base (e.g., Fouch and Dean, 1982; Mount, 1984). The green claystone was also deposited below wave base in relatively deep water, after the marl. That was followed by a shallowing-up transition to deposition of red mudstone with paleosols and thin sandstone beds in the advancing Colorado River delta, followed by the earliest through-going Colorado River channel sandstones and associated floodplain mudstones. The overlying, shallow-water, upper limestone unit records a return to a standing body of water, prior to the *second* arrival of the through-going Colorado River, recorded by the overlying and inset Bullhead Alluvium.

Sequence Stratigraphy

Analysis of changes in lithology, depositional energy, and processes through time allows us to interpret how changes in water level and sediment input influenced deposition of the Bouse Formation. This analysis applies well established principles of sequence stratigraphy, which provides a powerful tool for interpreting the stratigraphic

39

record of sedimentary basins (e.g., Vail et al., 1977; Posamentier et al., 1988, 1992; Van Wagoner et al., 1990; Posamentier and Allen, 1999; Plint and Nummedal, 2000; Catuneanu et al., 2009). Figure 19A illustrates the simplified unique arrangement of Bouse stratigraphic units in the study area. Figure 19B shows how we interpret two cycles of base level rise and fall, along with associated changes in water depth, from the systematic and well defined stratigraphic pattern seen in Figure 19A.
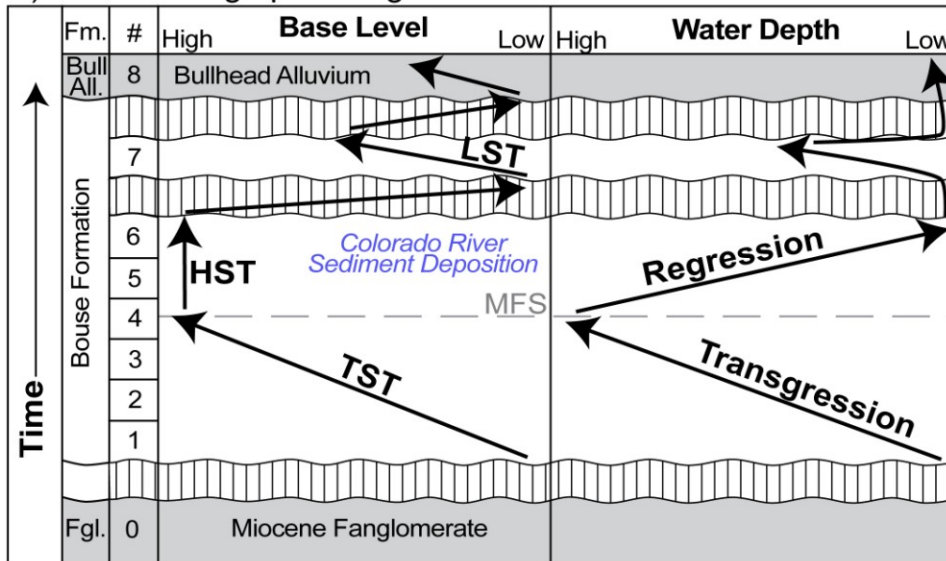
The Bouse Formation in the study area can be divided into two sequences bounded by erosional unconformities (Fig. 19A). The lower sequence consists of a transgressive systems tract (TST) comprising the basal cobble lag to middle of the green claystone, overlain by a highstand systems tract (HST – Colorado River mudstone and channel sandstone). The older units (1-6) are erosionally overlain and inset by the upper limestone (unit 7), which is the upper unconformity-bounded sequence of the Bouse Formation. Deposition of the oldest units, 1-4, occurred during widespread transgression and deepening-up that culminated in the maximum flooding surface (MFS) in the green claystone. The TST thus can be regarded as an overall fining-upward lower part of a sequence that records a progressive rise in base level and an increase in water depth, with the deepest water represented by the maximum flooding surface, MFS (e.g., Vail, 1987; Posamentier & Allen, 1999; Catuneanu et al., 2009). The MFS in the green claystone represents a turn-around point, which is followed by progressive shallowing-up and deposition of units 5 and 6, Colorado River red mudstone and cross-bedded channel sandstone.

It is important to note that water depth decreased and gave way to a fluvial channel and floodplain setting in the later part of the base-level highstand (units 5, 6) due
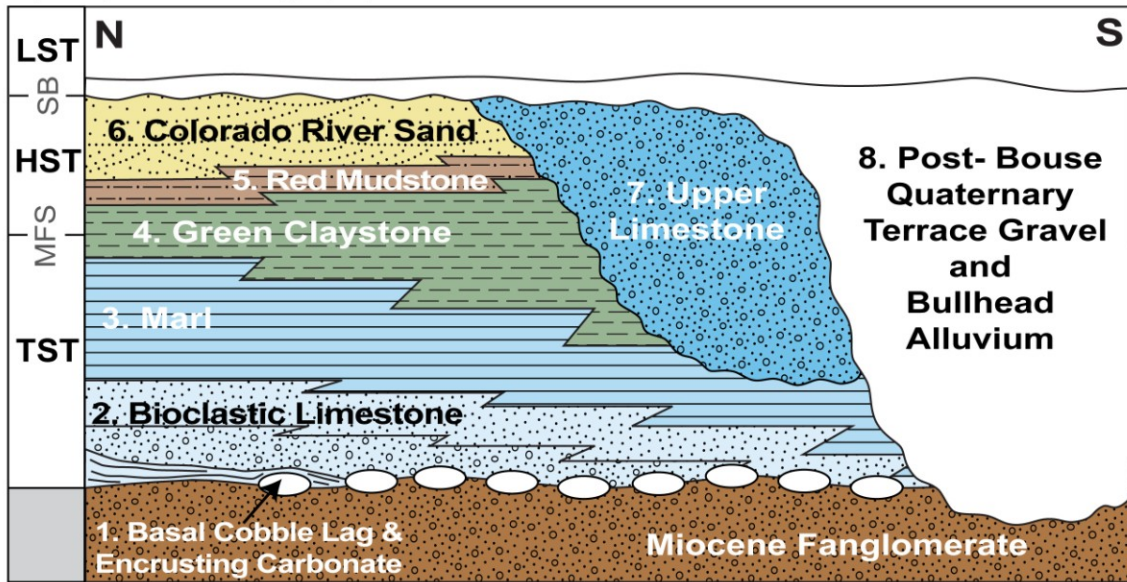
Figure 19. A) Generalized sequence stratigraphic cross-section of the Bouse Formation. TST - Transgressive Systems Tract; MFS – Maximum Flooding Surface; HST – Highstand Systems Tract; SB – Sequence Boundary; LST – Lowstand Systems Tract. B) Chronostratigraphic diagram of Bouse Formation base level and water depth changes through time. See previous (A) for abbreviation descriptions.

to progradation of Colorado River sediment into the basin during what is known as a

"normal regression" (e.g., Posamentier et al., 1988, 1992; Van Wagoner et al., 1990;

Posamentier & Allen, 1999; Catuneanu et al., 2009). We infer that a normal regression (defined as regression of the shoreline during base-level highstand due to high sediment supply) occurred during this highstand interval, rather than a forced regression, which is defined as forming during a falling stage system tract (FSST) due to base level lowering. This conclusion is based on the critical observation that the Colorado River sandstone everywhere conformably overlies the associated red mudstone fluvial floodplain deposits, which themselves conformably overlie the deep-water green claystone. Other than normal channelization within the red mudstone and Colorado River sandstone units, which is the expected result of autogenic (internally driven) lateral migration and avulsion of river channels, we never see an erosive sequence boundary at the base of the Colorado River sand unit, and it is never in contact with the deep-water green claystone. This important relationship requires a continued highstand of base level (lake or marine estuary) that persisted during deposition of the Colorado River channel sandstone (unit 6) (e.g., Posamentier et al., 1992; Catuneanu et al., 2009).

Following the HST there was a period of non-deposition and erosion that formed an erosional sequence boundary caused by lowering of base level for a period of time. This was then followed by deposition of the upper limestone, unit 7, during a rise in base level that caused resumption of deposition in a standing body of water (lake or marine estuary) and related establishment of a new carbonate faunal community that included gastropods, bivalves, barnacles, and calcareous algae. The upper limestone thus records a return rise in base level and water depth after a lowstand and period of erosion, as the basin was again filled by a standing body of water. Finally, there was another base-level

drop and decrease in water depth during a final period of erosion, before fluvial base

level rose again to deposit the Bullhead Alluvium (Fig. 19).

Syn-Depositional Tilting and Tectonic Implications

Detailed analysis of stratigraphic architecture in the Cibola area reveals gentle

dips with systematic wedging and westward thickening of well-defined units in the Bouse

Formation, as seen in Figures 13 and 14. The restored facies panels (Figs. 13B, 14B) are

hung from the youngest laterally extensive datums (base of red mudstone and base of

marl 2), which removes post-datum tilting and illustrates internal stratal geometries that

existed during deposition of the Bouse in this area. The origin of unit thickening and

gentle dips can be interpreted by considering several hypothetical stratal geometries that

could have formed during deposition and base level rise (Fig. 20).
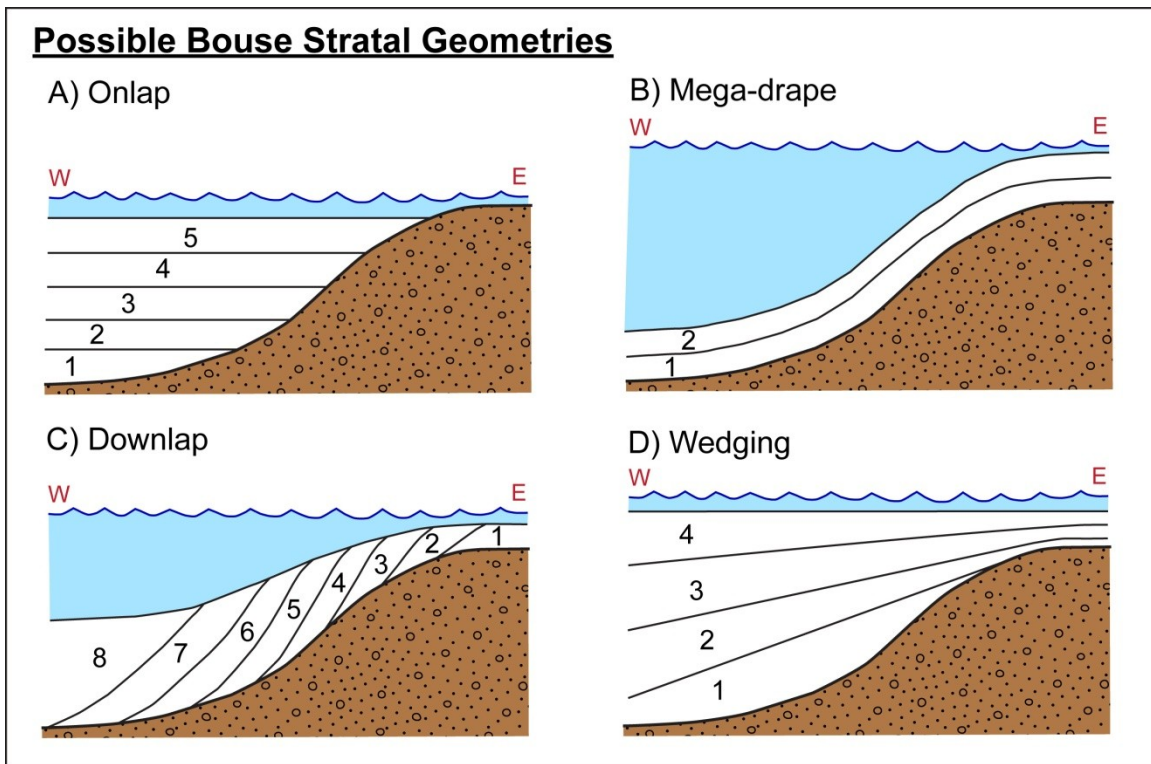
Figure 20. Proposed possible Bouse stratal geometries. Numbers indicate relative geologic age, with 1 being the oldest. A) Onlap geometry. B) Mega-drape geometry. C) Downlap geometry. D) Wedging geometry.

The first hypothetical stratal geometry shows the pattern known as "onlap" (e.g., Catuneanu et al., 2009), produced by deposition of horizontal units that would terminate against steeper, previously deposited Miocene fanglomerate (e.g., Buising, 1990). Recent studies that assign younger ages to higher-elevation exposures of the Bouse (Roskowski et al., 2010; McDougall and Miranda-Martinez, 2014) suggest bedding dips that are gentler than local topography and include an unstated assumption that the Bouse stratal architecture resembles the onlap geometry in Figure 20A. The second hypothetical geometry is a large "mega-drape" of sediment that overlies and mimics pre-existing paleotopography (Fig. 20B), as suggested for the northern Bouse Formation by House et al. (2005, 2008). The third hypothesis, downlap (Fig. 20C), consists of stratal units with a primary dip formed by progradation or biological outward growth, in which initially inclined units terminate down-dip against the contact with underlying Miocene fanglomerate. The fourth hypothesis (Fig. 20D) is a wedging stratal geometry in which units thicken basinward and pinch out gradually landward, toward the basin margin. This geometry suggests deposition of initially horizontal units that become progressively tilted during and after deposition. This hypothesis was originally suggested by Metzger (1968:D126), who noted, "The Bouse Formation is mostly flat lying, or has gentle dips. Locally, it is warped upward near the present-day mountains."

Most prevailing models of the Bouse Formation conclude that the present-day basin geometry of the lower Colorado River valley was acquired during pre-Bouse Miocene extensional and strike-slip deformation (Sherrod and Tosdal, 1991; Richard, 1993; Ricketts et al., 2011), and that the observed gentle dips in the Bouse are primary dips produced by deposition on pre-existing inclined surfaces (e.g., Spencer and Patchett,

44

1997; House et al., 2008; Spencer et al., 2008). However, the systematic westward thickening, wedging, and related eastward pinchout-of Bouse units in the Cibola area (Figs. 13, 14) most closely resemble the hypothetical stratal-wedging geometry in Figure 20D. This pattern is distinctly different than stratal geometries required by a static un-deformed Bouse basin, and instead appears to record progressive basinward tilting during deposition of the Bouse limestone and green claystone (units 1-4) for which we have reliable datums. The consistency of observed gentle basinward dips in the upper units (5-7) with syn-depositional dips in the lower 4 units further suggests that tilting continued at a slow rate during and after deposition of all units in the Bouse Formation.

Based on the above evidence for syn- to post-depositional basinward tilting in the Cibola area, combined with recognition of numerous post-Bouse faults and broad basinal geometry represented by surface and subsurface deposits (Metzger, 1968; Metzger et al., 1973; Sherrod and Tosdal, 1991; Richard, 1993), we propose a "sag basin" model for the Bouse Formation in the southern paleo-lake Blythe region (Fig. 1). Sag basins are a type of broad sedimentary basin in which the basin margins are defined by gentle dips toward the basin center and gradual pinch-out of units toward adjacent highlands (e.g., Platt and Wright, 1991; and Sylvester, 1999a). Unlike rift and strike-slip basins, sag basins are typically characterized by unfaulted basin margins, laterally continuous internal units, gentle dips over large areas, and a broadly downwarped basin center produced by syn-depositional diffuse extension and/or transtension (e.g., Platt and Wright, 1991; Nilsen and Sylvester, 1999a).

The observed systematic gentle dips, basinward thickening, landward pinch-outs of units, and prominent wedging geometry in the Cibola area (Figs. 13, 14) are most

consistent with a model for syn- to post-Bouse tilting or sagging across the basin (Fig. 20D). These observed geometries, when projected to the west, account for the full depth to deepest Bouse deposits beneath the modern Colorado River floodplain (>24 m below sea level) (Metzger et al., 1973). Syn-depositional (syn-Bouse) tilting is indicated by the features identified in units 2-4, and post-depositional tilting is indicated by consistent dips in Colorado River sands and overlying upper limestone (units 5-7). Similar stratal geometries produced by broad warping and subsidence over large areas are observed in other sag-rift and sag-transtensional basins such as the northern Teruel Graben, Spain (Alonso-Zarza and Calvo, 2000), and the Brunner Coal Beds in New Zealand (Titheridge, 1993). Gently tilted and wedging stratal geometries also commonly form in fault-bounded rift and strike-slip basins at the unfaulted margins of these basins, such as hanging-wall dip slope of an asymmetric half-graben (e.g., Schlische, 1995; Nilsen and Silvester, 1999b; Brothers et al., 2009).

Recognition of syn-depositional tilting in the Bouse Formation has regional implications for basin evolution and tectonics during Bouse deposition. As discussed above, the Laguna Fault system accommodated regional transtensional deformation related to dextral strike-slip faulting in the ECSZ during late Miocene time, ca. 12-6 Ma, during reorganization of the Pacific-North American plate boundary to form the modern San Andreas Fault system (Fig. 1; Sherrod and Tosdal, 1991; Richard, 1993; Glazner et al., 2002; Howard and Miller, 1992; Jachens and Howard, 1992; Ricketts et al., 2011). Based on this background, two conclusions can be made: (1) Tilting or sagging during deposition of the Bouse likely occurred due to the diffuse transtensional nature of the Laguna Fault system which caused broad basin subsidence, suggesting that slow strain in

this fault system continued during and after late Miocene time. (2) Based on recognition of faults that cut the Bouse and pre-date the Bullhead Alluvium (Fig. 17), we know the region was still tectonically active during Bouse deposition. We infer that this phase of slow transtensional strain with locally active faults was ongoing during latest Miocene to earliest Pliocene time, and that this resulted in a broad basinal sag in the southern Blythe paleolake.

Upper Limestone of the Bouse Formation

Contradictory ages have been proposed for the timing of the first through-going Colorado River and its earliest connection to the Gulf of California. Some studies (e.g. Spencer et al., 2013) suggest that the river first flowed through this region to the sea after 4.8 Ma, after Bouse deposition, based on the age of the interbedded Lawlor tuff within the Bouse Formation at Buzzard's Peak. Other studies (Dorsey et al., 2007, 2011) propose that appearance of 5.3 Ma Colorado River sand in the Salton Trough provides a record of the first through-going Colorado River half-a-million years earlier, depositing sediment in the Salton Trough during Bouse deposition. A maximum age for the Bouse Formation is provided by the 5.6 Ma tuff of Wolverine Creek, which underlies and slightly pre-dates the Bouse in the north near Bullhead City (House et al., 2008).

In this study, we identify an upper limestone unit that has not been recognized in previous studies of the Bouse Formation. The upper limestone (unit 7) is observed in the Palo Verde composite section (Fig. 16) and middle Cibola facies panel (Fig.13), where it overlies thick exposures of Colorado River channel sands and interbedded fluvial floodplain deposits. We conclude that unit 6 represents the earliest through-going Colorado River based on the presence of floodplain mudstones with mudcracks and

47

paleosols, and thick (up to 3 m), multistory, trough cross-bedded channel sandstones indicating the presence of deep fluvial channels that migrated across a broad fluvial floodplain during base-level rise and aggradation. Furthermore, we propose that the upper limestone is roughly equivalent in age to the limestone at Buzzard's Peak (4.8 Ma), which would bracket the age of the first through-going Colorado River between 5.6 and 4.8 Ma, consistent with an age of 5.3 Ma determined from stratigraphic studies in the Salton Trough (Dorsey et al., 2007, 2011). We further propose that the upper limestone records a second re-flooding event (Fig. 19) by either a lake or marine estuary. This chronology solves the longstanding age problem for the earliest transit of a through-going river down the Colorado River valley to the Gulf of California.

By reconciling datasets that were previously considered to be contradictory, we can speculate that deposition of the Bouse Formation in paleolake Blythe may have started ~5.6-5.5 Ma and lasted about 200-300 ka. This duration is consistent with estimates for the duration of Bouse deposition based on extrapolation of calculated accumulation rates in laminated marl to the entire thickness of the Bouse Formation (Fig. 18). According to this hypothesis, the first-arriving Colorado River prograded through the southern paleo-lake Blythe and delivered sand as turbidites to the marine basin in the Salton Trough at ca. 5.3 Ma. We infer that initial through-put of river sand was followed by a re-flooding episode (second Bouse highstand) and deposition of the upper limestone unit at ~4.8 Ma. This episode was followed by a second lowstand which formed the next sequence-bounding unconformity and delivered the second arrival of the Colorado River, recorded in younger deposits of the Bullhead Alluvium.

The proposed sequence of events reconciles previous, contradictory hypotheses for the age of the first through-going Colorado River (Dorsey et al., 2007, 2011; Spencer et al., 2013). This chronology is consistent with stratigraphic relations in the Salton Trough, which provide evidence for a ~200 ka hiatus after initial input of Colorado River-derived sand at 5.3 Ma, prior to voluminous sediment input and progradation of the Colorado River delta into the Salton Trough starting ca. 4.8 Ma (Dorsey et al., 2007, 2011). During the hiatus in the Salton Trough (5.1 to 4.9 Ma), sediment of the Colorado River may have been trapped upstream due to re-establishment of a tectonic paleodam that blocked the river and caused the second flooding event that deposited the upper limestone. Alternatively, the upper limestone may have been deposited during a highstand of relative sea level due to either a global eustatic sea level rise (Miller et al., 2005) or accelerated subsidence in the basin, in which case an intermittent paleodam would not be necessary. Regardless of whether re-flooding of paleo-lake Blythe was controlled by an intermittent paleodam (in a lake interpretation) or changes in relative sea level (in a marine estuary), recognition of the upper limestone is a critical new step toward resolution of a long-standing controversy over the age of earliest integration of the Colorado River to the ocean.

CHAPTER VI

CONCLUSIONS

In this study we have combined detailed measured sections, sedimentary lithofacies descriptions, and stratigraphic analysis to reconstruct the evolution and depositional history of the Bouse Formation in the southern paleo-lake Blythe along the lower Colorado River. The main conclusions of this study are summarized below.

(1) Application of sequence stratigraphic concepts and systems tract analysis reveals two full cycles of base level rise and fall during Bouse deposition that coincide with two cycles of transgression and regression. The lower sequence consists of a basal cobble lag, basal limestone (bioclastic carbonate and marl), green claystone, red mudstone, and Colorado River fluvial channel sandstone with floodplain muds. The upper sequence, identified for the first time in this study, consists of an upper bioclastic limestone unit that rests unconformably on most units of the lower sequence.

(2) Our data do not resolve a long-standing controversy over the depositional environment of the Bouse. However, we recognize an abrupt stratigraphic transition from carbonate marl to green claystone that coincides with shifts in micropaleontology and stable isotopes suggesting a change from marine-estuary to lacustrine conditions (Bright et al., 2014; McDougall and Miranda-Martinez, 2014). This change may have resulted from a large increase in water discharge of the newly arriving Colorado River. This is a new idea that needs to be tested in future studies.

(3) Detailed facies panels near Cibola, Arizona, provide evidence for syn- to post-depositional basinward tilting, leading us to propose a "sag basin" model for regional subsidence during deposition of the Bouse. This model is consistent with existing

50
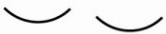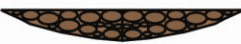
information about the style and timing of regional faults, and helps explain several new observations of faults that cut the Bouse and are overlapped by the younger Bullhead Alluvium. We thus conclude that the Bouse Formation accumulated in a broad sag basin during a period of transtensional strain in the Laguna Fault system.

(4) Recognition of the upper limestone unit resolves a long-standing debate over the age of the first through-going Colorado River. According to our chronological model, deposition of the basal limestone and green claystone took place sometime between 5.6 and 5.3 Ma, and the cross-bedded channel sandstone unit was deposited in the earliest through-going Colorado River from ~ 5.3 to 5.1 Ma. This was followed by re-flooding of the basin and deposition of the upper limestone between about 5.1 and 4.8 Ma during a previously documented hiatus in delivery of sand to the Salton Trough. The re-flooding episode may have been caused by either damming of the river by a tectonically controlled paleodam (in the lake model), or a rise in relative sea level due to a rise in global sea level or acceleration of tectonic subsidence (in the marine-estuary model). Finally, deposition of the Bullhead Alluvium records re-establishment of the through-going Colorado River after ~ 4.8 Ma.

APPENDIX A

BOUSE FORMATION MEASURED SECTIONS

Sedimentary Structures and Symbols

Symbol	Description
	Barnacle Encrusted Clasts
	Pebbles and Cobbles
	Mud Rip-Up Clasts
	Oscillatory Wave Rippled Beds
	Trough Cross Bedding
	Hummocky Cross Bedding
	Ripple Cross Bedding
	Cross Stratification
	Barnacles/Barnacle Rich Beds
	Barnacle Oncoids
	Stromatilitic/Algal Encrusted Clasts
	Coralline Green Algae
	Tufa
	Fossils including Clams, Gastropods, and/or Ostracods
	Dessication Cracks
	Bioturbation
	Burrows
	Channel Fill
	Point Bar
	Calcarenite or Sandstone Lenses

Section A1

Section A2

Section A3

Section A5

Section A6a-e

A6e

A6d

A6c

HB13-67

A6c
A6a

Clay Silt Fine Sand Med. Sand Coarse Sand V. C. Sand Granule Pebble Cobble Boulder

Section A7

Section A9

HB13-70

Clay Silt Fine Sand Med. Sand Coarse Sand V. C. Sand Granule Pebble Cobble Boulder

Section A10

HB13-72

Clay Silt Fine Sand Med. Sand Coarse Sand V. C. Sand Granule Pebble Cobble Boulder

Section A11

Section A12

Section A13

Section A14

HB14-12

Clay Silt Fine Sand Med. Sand Coarse Sand V. C. Sand Granule Pebble Cobble Boulder

Section A15

Section A16

Section A17

Section A18

Section A19

Section A20

A20d
A20c

HB14-2
A20c

A20b

A20a

HB14-1

Clay Silt Fine Sand Med. Sand Coarse Sand V. C. Sand Granule Pebble Cobble Boulder

Section A21

Section A22

HB14-3

Clay   Silt   Fine Sand   Med. Sand   Coarse Sand   V. C. Sand   Granule   Pebble   Cobble   Boulder

Section A23

HB14-13

Clay Silt Fine Sand Med. Sand Coarse Sand V. C. Sand Granule Pebble Cobble Boulder

Section A24

Section A25

HB14-25

HB13-2

HB14-24

Clay Silt Fine Sand Med. Sand Coarse Sand V. C. Sand Granule Pebble Cobble Boulder

77

Section C2

Section C3

Section C4a & b

HB13-10

C4b / C4a

Clay Silt Fine Sand Med. Sand Coarse Sand V. C. Sand Granule Pebble Cobble Boulder

12
10
8
6
4
2
0

Section C5

Section C6

Section C7

HB13-14

Clay Silt Fine Sand Med. Sand Coarse Sand V. C. Sand Granule Pebble Cobble Boulder

Section C8

Section C9

Section C10

HB13-19

Section C11

Section C12

HB13-30

HB13-29

HB13-28

HB13-27

HB13-31

Clay Silt Fine Sand Med. Sand Coarse Sand V. C. Sand Granule Pebble Cobble Boulder

Section C13

HB13-20

HB13-21

Clay Silt Fine Sand Med. Sand Coarse Sand V. C. Sand Granule Pebble Cobble Boulder

Section C15

Section C16

Section C17

HB13-26

Clay Silt Fine Sand Med. Sand Coarse Sand V. C. Sand Granule Pebble Cobble Boulder

Section C18

Section C19

HB13-48
HB13-47
HB13-46
HB13-45
HB13-44
HB13-43
HB13-42
HB13-41
HB13-40
HB13-39
HB13-38
HB13-37

Clay Silt Fine Sand Med. Sand Coarse Sand V. C. Sand Granule Pebble Cobble Boulder

Section C20

HB14-23
HB14-22

Clay Silt Fine Sand Med. Sand Coarse Sand V. C. Sand Granule Pebble Cobble Boulder

Section C21a & b

HB13-52

HB13-51

C21b
―――
C21a

HB13-50

Clay
Silt
Fine Sand
Med. Sand
Coarse Sand
V. C. Sand
Granule
Pebble
Cobble
Boulder

Section C22

HB13-53

Clay Silt Fine Sand Med. Sand Coarse Sand V. C. Sand Granule Pebble Cobble Boulder

Section C23

HB13-24 & 25

HB13-36

HB13-23

Clay Silt Fine Sand Med. Sand Coarse Sand V. C. Sand Granule Pebble Cobble Boulder

Section C24

HB14-14

HB14-7
HB14-8

Clay | Silt | Fine Sand | Med. Sand | Coarse Sand | V.C. Sand | Granule | Pebble | Cobble | Boulder

Section C25

Clay Silt Fine Sand Med. Sand Coarse Sand V. C. Sand Granule Pebble Cobble Boulder

Section C26

Section C27

HB14-18

HB14-17

Clay · Silt · Fine Sand · Med. Sand · Coarse Sand · V. C. Sand · Granule · Pebble · Cobble · Boulder

Section C28

APPENDIX B

BOUSE FORMATION MEASURED SECTION DATA

Section Name	UTM		Latitude	Longitude	Thickness (m)
	Northing	*Easting*			
A1	3682348	719678	33.257778	-114.64177	22.9
A2	3682088	719799	33.25541	-114.640535	17.0
A3	3682485	718395	33.259274	-114.6555	9.7
A4	3684041	718535	33.273268	-114.653623	13.65
A5	3683699	720577	33.26977	-114.631798	13.0
A6-a	3683722	720473	33.269998	-114.632908	3.2
A6-b	3683673	720168	33.269619	-114.636192	N/A
A6-c	3683689	720056	33.269786	-114.63739	8.6
A6-d	3683694	719930	33.269857	-114.63874	10.15
A6-e	3683672	719864	33.269672	-114.639454	19.4(total)
A7	3685094	720588	33.282339	-114.63134	8.2
A8	3684274	719341	33.275204	-114.644919	25.8
A9	3687552	722476	33.304102	-114.610478	20.2
A10	3686991	721667	33.299214	-114.619298	13.2
A11	3686319	720922	33.293311	-114.627458	11.0
A12	3686534	721200	33.295191	-114.624422	8.1
A13	3686317	721124	33.293251	-114.62529	11.8
A14	3686549	719648	33.295645	-114.641073	22.8
A15	3686009	720202	33.290665	-114.63526	22.35
A16	3687382	721478	33.302776	-114.621231	8.95
A17	3687022	720742	33.299683	-114.629218	21.6
A18	3685473	721467	33.285574	-114.621816	10.9
A19	3683785	719524	33.27076	-114.643074	26.4
A20-a	3682916	719890	33.262854	-114.639358	7.7
A20-b	3682956	719947	33.263202	-114.638737	9.9
A20-c	3683026	719959	33.263831	-114.638591	16.0
A20-d	3683062	720051	33.264136	-114.637596	30.4(total)
A21	3682666	720375	33.260501	-114.634216	23.75
A22	3682432	719340	33.258604	-114.645376	13.75
A23	3686530	719629	33.295477	-114.641282	38.9
A24	3686021	719936	33.290827	-114.638111	27.7
A25	3683708	720445	33.269878	-114.633212	17.1

C1	3682399	711436	33.259888	-114.730174	10.2
C2	3681770	710907	33.254322	-114.735996	6.5
C3	3681895	711111	33.255409	-114.733778	5.6
C4-a	3681798	711106	33.254536	-114.733854	7.55
C4-b	3681780	711135	33.254368	-114.733547	10.65 (total)
C5	3681666	710937	33.253379	-114.735698	1.43
C6	3682069	710741	33.25705	-114.737707	2.7
C7	3681640	709869	33.253353	-114.747161	9.25
C8	3681436	709171	33.25165	-114.754695	13.9
C9	3681436	708716	33.251739	-114.759576	4.65
C10	3681324	706385	33.251178	-114.784607	4.35
C11	3681366	707305	33.25138	-114.774728	5.65
C12	3681248	708647	33.250058	-114.76036	10.55
C13	3680744	704426	33.246324	-114.805753	9.45
C14	3680691	704464	33.245839	-114.805357	2.85
C15	3681277	706723	33.25069	-114.780992	8.3
C16	3681384	706912	33.251618	-114.77894	4.2
C17	3681393	707685	33.25155	-114.770646	7.4
C18	3692605	711623	33.351836	-114.72578	9.85
C19	3681383	707936	33.251412	-114.767956	11.55
C20	3685929	708128	33.292348	-114.764852	20.7
C21-a	3686353	707928	33.296209	-114.766901	5.8
C21-b	3686324	708023	33.295929	-114.765888	16.6(total)
C22	3686261	708131	33.29534	-114.764743	7.72
C23	3681705	707332	33.254431	-114.774361	12.15
C24	3682529	708493	33.261633	-114.761717	18.8
C25	3683086	709764	33.266407	-114.747953	11.45
C26	3682537	710145	33.261384	-114.743992	11.2
C27	3679859	703018	33.238614	-114.821054	3.65
C28	3686403	709360	33.296381	-114.75152	18.9

APPENDIX C

BOUSE FORMATION SAMPLE DATA

Sample	UTM Northing	UTM Easting	Latitude	Longitude	Measured Section	Height in M.S. (m)	Facies
Moabi13-3	3844813	728223	34.719892	-114.507713	N/A		Grn. Claystone
DB13-1B					N/A		Tufa
DB13-2	3740356	728130	33.778747	-114.536327	N/A		Grn. Claystone
DB13-4	3682455	711396	33.2604	-114.73059	N/A		Grn. Claystone
HB13-1	3683666	720162	33.269557	-114.636258	N/A		Marl
HB13-2	3683743	720546	33.270172	-114.63212	A25	13.1	Upper L.S. Bry
HB13-3	3682398	711435	33.259879	-114.730185	N/A		Clams frm Marl
HB13-4	3682455	711396	33.2604	-114.73059	C1	3.15	Varved Marl
HB13-5	3671010	699011	33.159598	-114.865971	N/A		Tufa
HB13-6	3682399	711436	33.259888	-114.730174	C1	1.0	Varved Micrite
HB13-7	3682399	711436	33.259888	-114.730174	C1	4.8	Grn. Claystone
HB13-8	3682399	711436	33.259888	-114.730174	C1	9.8	Bullhead Qtzt
HB13-9	3681818	710997	33.254737	-114.735019	N/A		Clam Marl
HB13-10	3681780	711135	33.254368	-114.733547	C4-b	9.9	Calcarenite
HB13-11	3681736	711195	33.253959	-114.732914	N/A		Fossil Hash
HB13-12	3681237	709951	33.249705	-114.746374	N/A		Micrite
HB13-13	3681689	710458	33.25368	-114.740831	N/A		Grn. Claystone
HB13-14	3681640	709869	33.253353	-114.747161	C7	1.5	Varved Micrite
HB13-15	3681436	709171	33.25165	-114.754695	C8	1.3	Calcarenite
HB13-16	3681436	709171	33.25165	-114.754695	C8	3.5	Calcarenite
HB13-17	3681436	709171	33.25165	-114.754695	C8	7.4	Marl
HB13-18	3681553	708868	33.252764	-114.757919	N/A		Varved Marl
HB13-19	3681324	706385	33.251178	-114.784607	C10	3.95	Fossil Hash
HB13-20	3680744	704426	33.246324	-114.805753	C13	8.4	Upper L.S. Clm
HB13-21	3680744	704426	33.246324	-114.805753	C13	1.1	Barnacle Marl
HB13-22	3692696	711420	33.352696	-114.727939	N/A		Tufa/Algal Mnd
HB13-23	3681705	707332	33.254431	-114.774361	C23	5.0	Marl
HB13-24	3681755	707323	33.254883	-114.774446	C23	11.3	C.R. Sand
HB13-25	3681755	707323	33.254883	-114.774446	C23	11.3	C.R. Sand
HB13-26	3681393	707685	33.25155	-114.770646	C17	0.70	Reworked Sand
HB13-27	3681248	708647	33.250058	-114.76036	C12	3.2	Calcarenite
HB13-28	3681248	708647	33.250058	-114.76036	C12	9.0	Marl
HB13-29	3681248	708647	33.250058	-114.76036	C12	9.7	Marl
HB13-30	3681248	708647	33.250058	-114.76036	C12	10.5	Micrite
HB13-31	3681248	708647	33.250058	-114.76036	C12	0.90	Reworked Sand
HB13-32	3681500	708775	33.252304	-114.758929	N/A		Algal Mound
HB13-33	3681453	708706	33.251894	-114.75968	N/A		Algal Rhodolith
HB13-34	3681453	708706	33.251894	-114.75968	N/A		Algal Mound
HB13-35	3681453	708706	33.251894	-114.75968	N/A		Algal Mound
HB13-36	3681705	707332	33.254431	-114.774361	C23	10.0	Red Mudstone
HB13-37	3681383	707936	33.251412	-114.767956	C19	2.3	Marl
HB13-38	3681383	707936	33.251412	-114.767956	C19	2.8	Marl
HB13-39	3681383	707936	33.251412	-114.767956	C19	3.3	Marl
HB13-40	3681383	707936	33.251412	-114.767956	C19	3.8	Marl
HB13-41	3681383	707936	33.251412	-114.767956	C19	4.2	Marl
HB13-42	3681383	707936	33.251412	-114.767956	C19	4.6	Marl
HB13-43	3681383	707936	33.251412	-114.767956	C19	5.0	Marl
HB13-44	3681383	707936	33.251412	-114.767956	C19	5.5	Marl
HB13-45	3681383	707936	33.251412	-114.767956	C19	6.0	Marl
HB13-46	3681383	707936	33.251412	-114.767956	C19	6.45	Marl
HB13-47	3681383	707936	33.251412	-114.767956	C19	6.9	Fossil Hash
HB13-48	3681383	707936	33.251412	-114.767956	C19	7.4	Barnacle Marl
HB13-49	3685929	708128	33.292348	-114.764852	C20	float	Upper L.S.
HB13-50	3686353	707928	33.296209	-114.766901	C21-a	4.9	Tufa

HB13-51	3686324	708023	33.295929	-114.765888	C21-b	10.7	Tufa
HB13-52	3686324	708023	33.295929	-114.765888	C21-b	11.4	B. Oncoid Hash
HB13-53	3686261	708131	33.29534	-114.764743	C22	1.0	Grn. Claystone
HB13-54	3686807	708572	33.300176	-114.759884	N/A		Algal Mound
HB13-55	3686807	708572	33.300176	-114.759884	N/A		Algal Mound
HB13-56	3681676	708615	33.253921	-114.760605	N/A		Marl
HB13-57	3682348	719678	33.257778	-114.64177	A1	2.35	Reworked Sand
HB13-58	3682348	719678	33.257778	-114.64177	A1	2.8	Tufa
HB13-59	3682348	719678	33.257778	-114.64177	A1	3.8	Calcarenite
HB13-60	3682348	719678	33.257778	-114.64177	A1	6.75	Calcarenite
HB13-61	3682348	719678	33.257778	-114.64177	A1	10.45	Calcarenite
HB13-62	3682348	719678	33.257778	-114.64177	A1	12.0	Marl
HB13-63	3682348	719678	33.257778	-114.64177	A1	18.3	Fossil Hash
HB13-64	3684041	718535	33.273268	-114.653623	A4	9.7	Grn. Claystone
HB13-65	3684041	718535	33.273268	-114.653623	A4	12.2	Bullhead Sand
HB13-66	3684057	718620	33.273395	-114.652707	N/A		Varved Marl
HB13-67	3683672	719864	33.269672	-114.639454	A6-d	10.1	Marl
HB13-68	3685055	722527	33.281588	-114.610545	N/A		Hash Mounds
HB13-69	3684934	721749	33.280659	-114.618922	N/A		Clm Hash Mnd
HB13-70	3687552	722476	33.304102	-114.610478	A9	9.6	Bncle Clams
HB13-71	3687521	721605	33.304003	-114.619834	N/A		Algal Mound
HB13-72	3686991	721667	33.299214	-114.619298	A10	4.25	Fossil Hash
HB13-73	3686317	721124	33.293251	-114.62529	A13	2.1	Calcarenite
HB13-74	3686317	721124	33.293251	-114.62529	A13	4.3	Fossil Hash
HB13-75	3686317	721124	33.293251	-114.62529	A13	5.9	Calcarenite
HB13-76	3685324	721615	33.284201	-114.620264	N/A		Fossil Hash
HB14-1	3682916	719890	33.262854	-114.639358	A20-a	5.3	Marl
HB14-2	3683026	719959	33.263831	-114.638591	A20-c	10.6	Fossil Hash
HB14-3	3682432	719340	33.258604	-114.645376	A22	8.6	Marl
HB14-4	3681828	709421	33.255135	-114.751923	N/A		Varved Marl
HB14-5	3686202	706878	33.29505	-114.778205	N/A		Fossil Hash
HB14-6	3685850	708381	33.291587	-114.762155	N/A		C.R. Geode
HB14-7	3682529	708493	33.261633	-114.761717	C24	6.8	Bullhead Sand
HB14-8	3682529	708493	33.261633	-114.761717	C24	6.6	Bullhead Sand
HB14-9	3686414	709391	33.296474	-114.751185	N/A		Flt Carb. Nod.
HB14-10	3683708	720445	33.269878	-114.633212	A5	float	Upper L.S. Algae
HB14-11	3684996	720538	33.281466	-114.631901	N/A		Calcarenite
HB14-12	3686549	719648	33.295645	-114.641073	A14	14.1	C.R. Sand
HB14-13	3686469	719540	33.294946	-114.642252	A23	37.0	QTG Geode
HB14-14	3682529	708493	33.261633	-114.761717	C24	8.4	Bullhead Sand
HB14-15	3680744	704426	33.246324	-114.805753	C13	float	Upper L.S.
HB14-16	3680280	703873	33.242247	-114.811789	N/A		Algal Mound
HB14-17	3679859	703018	33.238614	-114.821054	C27	1.2	Oncoid Marl
HB14-18	3679859	703018	33.238614	-114.821054	C27	3.55	Upper L.S.
HB14-19	3686403	709360	33.296381	-114.75152	C28	8.2	Upper L.S.
HB14-20	3686403	709360	33.296381	-114.75152	C28	9.5	Upper L.S.
HB14-21	3686403	709360	33.296381	-114.75152	C28	14.1	Upper L.S.
HB14-22	3685929	708128	33.292348	-114.764852	C20	14.0	Upper L.S.
HB14-23	3685929	708128	33.292348	-114.764852	C20	14.4	Upper L.S.
HB14-24	3683708	720445	33.269878	-114.633212	A25	10.7	C.R. Sand
HB14-25	3683708	720445	33.269878	-114.633212	A25	13.5	Upper L.S.
HB14-26	3715070	736893	33.54898	-114.448512	N/A		Reworked Tuff

APPENDIX D

BOUSE FIGURE IMAGE DATA

Figure #	UTM		Latitude	Longitude	Measured Section
	Northing	Easting			
6A	3686298	708340	33.29563	-114.76249	N/A
6B	3692696	711420	33.3527	-114.72794	N/A
6C	3685324	721615	33.2842	-114.62026	N/A
6D	3686353	707928	33.29621	-114.7669	C21a
6E	3681487	710230	33.2519	-114.74332	N/A
6F	3681487	710230	33.2519	-114.74332	N/A
7A	3682348	719678	33.25778	-114.64177	A1
7B	3682530	719191	33.25952	-114.64695	N/A
7C	3686354	720823	33.29365	-114.62851	N/A
7D	3682348	719678	33.25778	-114.64177	A1
7E	3683672	719864	33.26967	-114.63945	A6e
7F	3681500	708775	33.2523	-114.75893	N/A
7G	3681324	706385	33.25118	-114.78461	C10
7H	3681384	706912	33.25162	-114.77894	C16
7I	3686324	708023	33.29593	-114.76589	C21b
7J	3686324	708023	33.29593	-114.76589	C21b
8A	3684041	718535	33.27327	-114.65362	A4
8B	3681705	707332	33.25443	-114.77436	C23
8C	3682088	719799	33.25541	-114.64054	A2
8D	3682399	711436	33.25989	-114.73017	C1
8E	3681553	708868	33.25276	-114.75792	N/A
9A	3686946	708560	33.30143	-114.75998	N/A
9B	3682399	711436	33.25989	-114.73017	C1
9C	3686009	720202	33.29066	-114.63526	A15
9D	3685837	708348	33.29148	-114.76251	N/A
10A	3682529	708493	33.26163	-114.76172	C24
10B	3686549	719648	33.29564	-114.64107	A14
10C	3686549	719648	33.29564	-114.64107	A14
11A	3685929	708128	33.29235	-114.76485	C20
11B	3680744	704426	33.24632	-114.80575	C13
11C	3685929	708128	33.29235	-114.76485	C20
11D	3685929	708128	33.29235	-114.76485	C20
11E	3685929	708128	33.29235	-114.76485	C20
17A	3683699	720577	33.26977	-114.6318	A5
17B	3682529	708493	33.26163	-114.76172	C24
17C	3686408	709403	33.29642	-114.75106	N/A
18	3682399	711436	33.25989	-114.73017	C1

REFERENCES CITED

Alonso-Zarza, A.M., Calvo, J.P., 2000, Palustrine sedimentation in an episodically subsiding basin: the Miocene of the northern Teruel Graben (Spain): Palaeogeography, Palaeoclimatology, Palaeoecology v. 160, p. 1–21.

Bartley, J.M., and Glazner, A.F., 1991, En echelon Miocene rifting in the southwestern United States and model for vertical-axis rotation in continental extension: Geology, v. 19, p. 1165–1168.

Bright, J., Cohen, A.S., Dettman, D.L., and Dorsey, R.J., 2014, Ostracode-based faunal and stable isotope data suggest a mixed marginal marine to stratified lacustrine waterbody interpretation for the southern Bouse Formation, AZ: Geological Society of America *Abstracts with Programs*. Vol. 46, No. 6, p. 639.

Brothers, D.S., Driscoll, N.W., Kent, G.M., Harding, A.J., Babcock, J.M., and Baskin, R.L., 2009, Tectonic evolution of the Salton Sea inferred from seismic reflection data: Nat. Geosci., v. 2(8), p. 581–584.

Buising, A.V., 1988, Depositional and Tectonic Evolution of the Northern Proto–Gulf of California and Lower Colorado River, as Documented in the Mio-Pliocene Bouse Formation and Bracketing Units, Southeastern California and Western Arizona [Ph.D. thesis]: Santa Barbara, University of California, 196 p.

Buising, A.V., 1990, The Bouse Formation and bracketing units, southeastern California and western Arizona: Implications for the evolution of the proto-Gulf of California and the lower Colorado River: Jour. Geoph. Res. 95:20,111-20,132.

Buising, A.V.,1993, Stratigraphic overview of the Bouse Formation and gravels of the Colorado River, Riverside Mountains, eastern Vidal Valley, and Mesquite Mountain areas, Calif, and Ariz. In: Sherrod, D.R., and Nielson, J.E. (eds.) Tertiary Stratigraphy of Highly Extended Terranes, California, Arizona, and Nevada, p. 165-170.

Catuneanu, O., Abreu, V., Bhattacharya, J.P., Blum, M.D., Dalrymple, R.W., Eriksson, P.G., Fielding, C.R., Fisher, W.L., Galloway, W.E., Gibling, M.R., Giles, K.A., Holbrook, J.M., Jordan, R., Kendall, C.G.St.C., Macurda, B., Martinsen, O.J., Miall, A.D., Neal, J.E., Nummedal, D., Pomar, L., Posamentier, H.W., Pratt, B.R., Sarg, J.F., Shanley, K.W., Steel, R.J., Strasser, A., Tucker, M.E., Winker, C., 2009. Toward the standardization of sequence stratigraphy. Earth Science Reviews 92, 1–33.

Crossey, L.J., Karlstrom, K.E., Pearce, J.L.*, and Dorsey, R., 2011, Geochemistry of springs, travertines and lacustrine carbonates of the Grand Canyon region over the past 12 million years-The importance of groundwater on the evolution of the Colorado River system, 2011, In Beard, L. S., Karlstrom, K.E., Young, R. E., and Billingsley, G. H., CREvolution 2-Origin and Evolution of the Colorado River System, Workshop Abstracts: U.S.G.S. Open-file Report 2011-1210:62-68.

Crossey, L.J., Karlstrom, K.E., Dorsey, R.J., and Pearce, J.L., 2013, Geochemistry of springs, travertines and lacustrine carbonates of the Grand Canyon region over the past 12 million years: The importance of groundwater in initiating downward integration of the Colorado River system. Geological Society of America Abstracts with Programs. Vol. 45, No. 7, p. 252.

Davis, G.A., and Lister, G.S., 1988, Detachment faulting in continental extension; perspectives from the Southwestern U.S. Cordillera. In: Processes in Continental Lithospheric Deformation (Ed. by S . P. Clark, B. C. Burchfiel and J. Suppe), Geological Society of America Special Paper, 218, p. 133-159.

Dorsey, R.J., and Becker, U., 1995, Evolution of a large Miocene growth structure in the upper plate of the Whipple detachment fault, northeastern Whipple Mountains, California. *Basin Research*, vol. 7, p. 151-163.

Dorsey, R.J., Fluette, A., McDougall, K., Housen, B.A., Janecke, S.U., Axen, G.J., and Shirvell, C.R., 2007, Chronology of Miocene-Pliocene deposits at Split Mountain Gorge, southern California: Arecord of regional tectonics and Colorado River evolution: Geology, v. 35, p. 57–60.

Dorsey, R.J., Housen, B.A., Janecke, S.U., Fanning, C.M., and Spears, A.L.F., 2011, Stratigraphic record of basin development within the San Andreas fault system: Late Cenozoic Fish Creek-Vallecito basin, southern California. Geol. Society America Bull., v. 123, p. 771-793.

Dorsey, R.J., Crossey, L.J., Cohen, A.S., Howard, K.A., Karlstrom, K.E., Bright, J., Homan, M.*, McDougall, K., and Retallack, G.J., 2013, Lake-estuary hypothesis for the Bouse Formation: New look at an old problem. Geological Society of America Abstracts with Programs. Vol. 45, No. 7, p. 253.

Fouch, T.D., and Dean, W.E., 1982, Lacustrine environments and associated clastic depositional environments, in: Scholle, P.A., and Spearing, D., Sandstone depositional environments: American Association of Petroleum Geologists, p. 87–114.

Glazner, A.F., Walker, J.D., Bartley, J.M., and Fletcher, J.M., 2002, Cenozoic evolution of the Mojave block of southern California, *in* Glazner, A.F., Walker, J.D., and Bartley, J.M., eds., Geologic Evolution of the Mojave Desert and Southwestern Basin and Range: Boulder, Colorado, Geological Society of America Memoir 195, p. 19–41.

Harvey, 2014, Zircon age and oxygen isotopic correlations between Bouse Formation tephra and the Lawlor Tuff. Geosphere, v. 10,p. 221–232.

House, P.K., Pearthree, P.A., Howard, K.A., Bell, J.W., Perkins, M.E., Faulds, J.E., and Brock, A.L., 2005, Birth of the lower Colorado River—Stratigraphic and geomorphic evidence for its inception near the conjunction of Nevada, Arizona, and California, in Pederson, J.L., and Dehler, C.M., eds., Interior Western United States: Boulder, Colorado, Geological Society of America Field Guide 6, p. 357–387.

House, P.K., Pearthree, P.A., and Perkins, M.E., 2008, Stratigraphic evidence for the role of lake spillover in the inception of the lower Colorado River in southern Nevada and western Arizona, *in* Reheis, M.C., Hershler, R., and Miller, D.M., eds., Late Cenozoic Drainage History of the Southwestern Great Basin and Lower Colorado River Region: Geologic and Biotic Perspectives: Geol. Soc. Am. Bull. Special Paper 439, p. 335-353.

Howard, K.A., and Miller, D.M., 1992, Late Cenozoic faulting at the boundary between the Mojave and Sonoran blocks: Bristol Lake area, California. In: Richard, S.M. (ed.) Deformation associated with the Neogene Eastern California Shear Zone, southwestern Arizona and southeastern California. Redlands, CA, San Bernardino County Museum Spec. Publ., p. 37-47.

Howard, K.A., Lundstrom, S.C., Malmon, D.V., and Hook, S.J., 2008, Age, distribution, and formation of late Cenozoic paleovalleys of the lower Colorado River and their relation to river aggradation and degradation, *in* Reheis, M.C., Hershler, R., and Miller, D.M., eds., Late Cenozoic Drainage History of the Southwestern Great Basin and Lower Colorado River Region: Geologic and Biotic Perspectives: Geol. Soc. Am. Special Paper 439, p. 391–410.

Ingersoll, R.V., and Rumelhart, P.E., 1999, Three-stage evolution of the Los Angeles basin, southern California: Geology, v. 27, p. 593–596, doi: 10.1130/0091-7613(1999)027<0593:TSEOTL>2.3.CO;2.

Jachens, R.C., and Howard, K.A., 1992, Bristol Lake basin: A deep sedimentary basin along the Bristol-Danby Trough, Mojave Desert. In: Reynolds, R.E. (ed.) Old Routes to the Colorado.

Lucchitta, I., 1972, Early history of the Colorado River in the Basin and Range Province. Geological Society of America Bulletin, v. 83, p. 1933–1948.

Lucchitta, I., 1979, Late Cenozoic uplift of the southwestern Colorado Plateau and adjacent LCR region. Tectonophysics, v. 61, p. 63–95.

Lucchitta, I., McDougall, K., Metzger, D.G., Morgan, P., Smith, G.R., and Chernoff, B., 2001, The Bouse Formation and post-Miocene uplift of the Colorado Plateau, In: Young, R.A., and Spamer, E.E. (eds.) The Colorado River: Origin and Evolution: Grand Canyon, Arizona, Grand Canyon Association Monograph 12, p. 173–178.

McDougall, K., 2008, Late Neogene marine incursions and the ancestral Gulf of California, In: Reheis, M.C., Hershler, R., and Miller, D.M. (eds.) Late Cenozoic drainage history of the southwestern Great Basin and lower Colorado River region: Geologic and biotic perspectives. Geological Society of America Special Paper 439, p. 355-373.

McDougall, K., and Miranda-Martinez, A.Y., 2014, Evidence for a marine incursion along the lower Colorado River corridor: Geosphere, v. 10, p. 1-28.

Metzger, D.G., 1968, The Bouse Formation (Pliocene) of the Parker-Blyth-Cibola Area, Arizona and California: U.S.G.S. Prof. Paper 600-D, p. D126-D136.

Metzger, D.G., Loeltz, O.J., and Irelan, B., 1973, Geohydrology of the Parker-Blythe-Cibola area, Arizona and California: U.S. Geological Survey Professional Paper 486-G, 130 p.

Miller, K.G., Kominz, M.A., Browning, J.V., Wright, J.D., Mountain, G.S., Katz, M.E., Sugarman, P.J., Cramer, B.S., Christie-Blick, N., and Pekar, S.F., 2005, The Phanerozoic record of global sea-level change: Science, v. 310(5752), p. 1293-1298.

Mount, J.F., 1984, Mixing of siliciclastic and carbonate sediments in shallow shelf environments: Geology, v. 12, p. 432-435.

Nielson, J.E., and Beratan, K.K., 1990, Tertiary basin development and tectonic implications, Whipple detachment system, Colorado extensional corridor, California and Arizona. Journal of Geophysical Research: Solid Earth (1978-2012), v. 95(B1), p. 599-614.

Nilsen, T.H., and Sylvester, A.G., 1999a, Strike-slip basins, part 1: *The Leading Edge*, v. 18, p. 1146-1150.

Nilsen, T.H., and Sylvester, A.G., 1999b, Strike-slip basins, part 2: *The Leading Edge*, v. 18, p. 1258-1267.

Olmsted, F.H., Loeltz, O.J., and Irelan, B., 1973, Geohydrology of the Yuma area, Arizona and California: Water resources of lower Colorado River-Salton Sea area. U.S. Geological Survey Professional Paper 486-H, 227 p.

Pederson, 2008, The mystery of the pre–Grand Canyon Colorado River—Results from the Muddy Creek Formation. *GSA Today*: v. 18, no. 3, p. 4-10.

Platt, N.H., and Wright, V.P., 1991, Lacustrine carbonates: facies models, facies distributions and hydrocarbon aspects, in: P Anadón, L Cabrera, K Kelts (Eds.), Lacustrine Facies Analysis, Special Publication International Association of Sedimentologists, vol. 13, p. 57–74.

Plint, A.G., and Nummedal, D., 2000, The falling stage systems tract: recognition and importance in sequence stratigraphic analysis; in Sedimentary Responses to forced regressions; D. Hunt and R. Gawthorpe, eds., Geological Society of London, Special Publications, 172, p. 1-17.

Posamentier, H.W., Jervey, M.T., and Vail, P.R., 1988, Eustatic controls on clastic deposition: I. Conceptual framework, in Wilgus, C.K., Hastings, B.S., Kendall, C.G.St.C., Posamentier, H.W., Ross, C.A., and Van Wagoner, J.C., eds., Sea-Level Changes: An Integrated Approach: Society of Economic Paleontologists and Mineralogists Special Publication 42, p. 109–124.

Posamentier, H.W., Allen, G.P., James, D.P., Tesson, M., 1992. Forced regressions in a sequence stratigraphic framework: concepts, examples, and exploration significance. American Association of Petroleum Geologists Bulletin 76, 1687–1709.

Posamentier, H.W., and Allen, G.P., 1999, Siliciclastic sequence stratigraphy-Concepts and Applications: SEPM Concepts in Sedimnetology and Paleontology, Tulsa, Okla., 210 p.

Potochnik, A.R., 2001, Paleogeomorphic evolution of the Salt River region: Implications for Cretaceous-Laramide inheritance for ancestral Colorado River drainage, in Young, R.A., and Spamer, E.E., eds., Colorado River, Origin and Evolution: Grand Canyon, Arizona, Grand Canyon Association Monograph 12, p. 17–22.

Poulson, S.R. and John, B.E. 2003, Stable isotope and trace element geochemistry of the basal Bouse Formation carbonate, southwestern United States: Implications for the Pliocene uplift history of the Colorado Plateau: Geol. Soc. America Bulletin v. 115, p. 434-444.

Richard, S.M., 1993, Palinspastic reconstruction of southeastern California and southwestern Arizona for the Middle Miocene: Tectonics, v. 12, no. 4, p. 830–854.

Ricketts, J.W., Girty, G.H., Sainsbury, J.S., Muela, K.K., Sutton, L.A., Biggs, M.A., and Voyles, E.M., 2011, Episodic growth of the Chocolate Mountains anticlinorium recorded by the Neogene Bear Canyon Conglomerate, southeastern California. Journal of Sedimentary Research, v. 81, p. 859-873.

Roskowski, J.A., Patchett, P.J., Spencer, J.E., Pearthree, P.A., Dettman, D.L., Faulds, J.E., and Reynolds, A.C., 2010, A late Miocene-early Pliocene chain of lakes fed by the Colorado River: Evidence from Sr, C, and O isotopes of the Bouse Formation and related units between Grand Canyon and the Gulf of California: Geol. Soc. Am. Bull. 122:1625-1636.

Sandberg. P.A., 1966. The modern ostracods Cyprideis bensoni, n. sp. Gulf of Mexico, and C. castus, Baja California. Journal of Paleontology, v. 40, p. 447-449.

Sarna-Wojcicki, A.M., Deino, A.L., Fleck, R.J., McLaughlin, R.J., Wagner, D., Wan, E., Wahl, D., Hillhouse, J.W., and Perkins, M., 2011, Age, composition, and areal distribution of the Pliocene Lawlor Tuff, and three younger Pliocene tuffs, California and Nevada. Geosphere, v. 7; p. 599-628.

Schlische, R.W., 1995, Geometry and origin of fault-related folds in extensional settings. Am. Assoc. Pet. Geol. Bull., 79, 1661–1678.

Shelef, E., and Oskin, M., 2010, Deformation processes adjacent to active faults: Examples from eastern California, J. Geophys. Res., 115, B05308, doi:10.1029/2009JB006289.

Sherrod, D.R., and Tosdal, R.M., 1991, Geologic setting and Tertiary structural evolution of southwestern Arizona and southeastern California. Journal of Geophysical Research, v. 96, p. 12,407-12,423.

Smith, P.B., 1970, New evidence for a Pliocene marine embayment along the lower Colorado River area, California and Arizona. Geol. Soc. Am. Bull. 81:1411-1420.

Spencer, J.E., and Reynolds, S.J., 1989, Tertiary structure, stratigraphy, and tectonics of the Buckskin Mountains. In: Geology and Resources of the Buckskin and Rawhide Mountains, West-Central Arizona (Ed. by J. E. Spencer and S. J. Reynolds), Bulletin of the Arizona Geological Survey, vol. 198, p. 103-167.

Spencer, J.E., and Patchett, P.J., 1997, Sr isotope evidence for a lacustrine origin for the upper Miocene to Pliocene Bouse Formation, lower Colorado River trough, and implications for timing of Colorado Plateau uplift. Geol. Soc. Am. Bull. 109:767-778.

Spencer, J.E., Peters, L., McIntosh, W.C., and Patchett, P.J., 2001, ^{40}Ar/^{39}Ar geochronology of the Hualapai Limestone and Bouse Formation and implications for the age of the lower Colorado River, In: Young, R.A., and Spamer, E.E., eds., The Colorado River: Origin and evolution: Grand Canyon, Arizona, Grand Canyon Association Monograph 12, p. 89-91.

Spencer, J.E., Pearthree, P.A., and House, P.K., 2008, An evaluation of the evolution of the latest Miocene to earliest Pliocene Bouse lake system in the lower Colorado River valley, southwestern USA, In: Reheis, M.C., Hershler, R., and Miller, D.M., eds., Late Cenozoic drainage history of the southwestern Great Basin and lower Colorado River region; geologic and biotic perspectives: Geol. Soc. Am. Bull. Special Paper 439:375-390.

Spencer, J.E., Patchett, P.J., Roskowski, J.A., Pearthree, P.A., Faulds, J.E., and House, P.K., 2011, A Brief review of Sr isotopic evidence for the setting and evolution of the Miocene-Pliocene Hualapai-Bouse lake system In: Beard, L.S., Karlstrom, K.E., Young, R.A., and Billingsley, G.H., eds., CREvolution 2—Origin and evolution of the Colorado River system, workshop abstracts: U.S. Geological Survey Open-File Report 2011-1210, p. 250-259.

Spencer, J.E., Patchett, P.J., Pearthree, P.A., and House, P.K., Sarna-Wojcicki, A.M., Wan, E., Roskowski, J.A., and Faulds, J.E., 2013, Review and analysis of the age and origin of the Pliocene Bouse Formation, lower Colorado River Valley, southwestern USA. Geosphere, v. 9, no. 3, p. 444-459.

Taylor, D.W., 1983, Late Tertiary mollusks from the Lower Colorado River valley: Ann Arbor, University of Michigan, Contributions from the Museum of Paleontology, v. 26, p. 289-298.

Titheridge, D.G., 1993, The influence of half-graben syn-depositional tilting on thickness variation and seam splitting in the Brunner Coal Measures, New Zealand. Sedimentary Geology, v. 87, p. 195–213.

Todd, T.N., 1976, Pliocene occurrence of the Recent atherinid fish Colpichthys regis in Arizona: Journal of Paleontology, v. 50, p. 462-466.

Vail, P.R., Mitchum Jr., R.M., Thompson III, S., 1977. Seismic stratigraphy and global changes of sea level, part 3: relative changes of sea level from coastal onlap. In: Payton, C.E. (Ed.), Seismic Stratigraphy — Applications to Hydrocarbon Exploration. Memoir, vol. 26. American Association of Petroleum Geologists, pp. 63–81.

Vail, P.R., 1987, Seismic stratigraphy interpretation procedure, in Bally, A.W. (ed.), Atlas of seismic stratigraphy: Am. Assoc. Petroleum Geology Studies in Geology 27, Vol. 1, p. 1-10.

Van Wagoner, J.C., Mitchum, R.M., Campion, K.M., and Rahmanian, V.D., 1990, Siliciclastic sequence stratigraphy in well logs, cores, and outcrops: AAPG Methods in Exploration Series 7, Am. Assoc. Petroleum Geologists, Tulsa, Okla., 55 p.

Winterer, J.L., 1975, Biostratigraphy of Bouse Formation: A Pliocene Gulf of California deposit in California, Arizona, and Nevada, M.S. thesis, Long Beach, California State University, 132 p.

Young, R.A., 1979, Laramide deformation, erosion and plutonism along the southwestern margin of the Colorado Plateau: Tectonophysics, v. 61, p. 25–47.